Integrated Master in Chemical Engineer

Feasibility of using a TiO_2 containing paint coat to inactivate microorganisms in an aqueous system

Master´s Dissertation

Of

Pablo Isaí Jiménez Calvo

Developed within the course of Dissertation

made in

Development Project on Academic Environment in LEPABE laboratory in collaboration with CIN, S.A. Enterprise.

Supervisor: Prof. Olga Nunes

Co-Supervisor: Prof. Adélio Mendes

Universidade do Porto
Faculdade de Engenharia
FEUP

Department of Chemical Engineering

January, 2014

For my Parents

"*Truth is ever to be found in simplicity, and not in the multiplicity and confusion of things.*" H. Hertz

Acknowledgement

First of all, I would like to thank God for creating and giving me an extraordinary opportunity to being abroad in a charming country as Portugal is.

Special gratitude to my Supervisor Professor Olga Nunes for accepting me in the first instance without any doubt to work on her side and show me the great world of microorganisms and any biological assistance I needed it. Also for her encouragement and guidance.

Special gratitude to my Co-Supervisor Professor Adélio Mendes for his encouragement and guidance and any help in the engineering facts that my work required along it is developed. And also to show me the great research field of photocatalysis.

I acknowledge the technical staff from Chemical Engineer Department (DEQ), who directly or indirectly help me out. I gratefully acknowledge Eng. Vera Sousa for sharing the knowledge, support, ideas and experimental techniques I needed to carry on this academic-professional aim. For making easy my adaptation in the lab environment.

I gratefully acknowledge Eng. Pedro Magalhães, Eng. Joana Ângelo and Eng. Roberto Magalhães for their kind technical assistance. The research group of the laboratory E009B, especially PhD. Ana Rita Lopes, MSc. Ana Mafalda Paiva and Lic. Ana Reis, whom supported me and encouraged me every time I needed, for the easy integration they provided me and made me part of social activities.

Special thanks to Dr. Gilberto Piedra for overseeing some parts of this project. Also, thanks to Eng. Javier Rodríguez for theoretical-practical engineering advices.

I deeply thank my mother, Aurora Calvo, and my father, Gerardo Jiménez, for the unconditional-priceless love, care and support through my life. Thank you both for being my mentors. Besides, my family members whom supported me and communicated me frequently.

To CIN S.A. which provided me paint material.

"To MICIT (Ministry of Science and Technology of Costa Rica) and CONICIT (National Council for Scientific and Technological Research), institutions that provided financial support during the Master Program".

Resumo

A população mundial deverá aumentar entre 40-50 % nos próximos 50 anos. Consequentemente, o aumento da demanda de água irá agravar a sua escassez [1]. A desinfecção de água potável é obtida usando desinfectantes químicos, tal como o cloro, dióxido de cloro ou ozono [2]. Estes populares métodos aplicam produtos químicos agressivos que, no entanto, têm um curto período de actividade [3]. Dado o risco das infecções poderem ser transmitidas através da água potável contaminada, é prioritário o desenvolvimento de novos sistemas de desinfecção. A fotocatálise com TiO_2 é um promissor tratamento de desinfecção devido à actividade bactericida deste composto [1]. Na presença de UV-A e oxigénio, o TiO_2 produz radicais livres altamente reativos, como o hidróxilo e o superóxido,$OH^{\bullet}$ e $O_2^{\bullet -}$, respectivamente.

O uso de nanopartículas em tecnologias de tratamento de água tem vindo a aumentar nos últimos anos. Entre 2008 e 2015, o volume de negócios para este tipo de aplicações deverá aumentar \$ $2.9x10^9$, um setor que provavelmente será liderado pelos EUA, Alemanha, Japão e China [4]. Para este mesmo período, prevê-se que a produção de nanopartículas de dióxido de titânio deverá atingir as 10^4 toneladas/ano [5].

Neste estudo foi testado um sistema fotocatalítico em contínuo, baseado numa malha porosa revestida com uma tinta fotocatalítica incorporando 9 % de TiO_2. Dois materiais de malha de arame foram testados, um de plástico e outro de aço inoxidável. Os ensaios de fotoinativação foram realizados com suspensões de *Escherichia coli* DSM 1103 (bactéria Gram-negativa) com uma densidade inicial de 1×10^6 mL^{-1}, com um caudal de 2 $mL \bullet s^{-1}$ durante 40 min.

Perdas de viabilidade de 54,1 % e 39,4 % foram obtidas para o aço inoxidável, 2 x 2 mm^2 e 3 x 3 mm^2, respectivamente após 40 min de irradiação. O efeito da área de superfície é importante uma vez que determina a quantidade de TiO_2 disponível para formar os radicais necessários para inactivar as bactérias. Uma perda de viabilidade de 89,4 % foi obtida em 80 min de irradiação. Estes resultados indicam uma possível relação linear entre tempo de irradiação e de inactivação e uma eficiente combinação do processo e do sistema contínuo na fotoinativação de *E. coli*. Os resultados deste estudo preliminar sugerem que esta tecnologia poderá ser melhorada no futuro.

Palavras Chave: fotocatálise, desinfecção da água

Abstract

The world´s population is expected to increase by 40-50 % within the next 50 years. Consequently, the increased water demand exacerbates the scarcity of clean water [1]. Drinking water disinfection is achieved by a chemical disinfectant, which is usually a powerful oxidizing agent such as chlorine, chlorine dioxide or ozone [2]. These popular disinfection methods often use aggressive chemicals and are not able to stay effective for long periods of time [3]. Given the risk that infections may be transmitted by contaminated drinking water, it is important to develop new disinfection systems. TiO_2-photocatalysis, is a promising water-disinfection treatment because of its bactericidal activity [1]. In the presence of UV-A and oxygen, TiO_2 produces highly reactive free radicals like hydroxyl and superoxide radicals, $OH^{\cdot}$ and $O_2^{\cdot -}$ respectively.

The use of nanoparticules in water treatment technologies has been increasing in latest years. Between 2008 and 2015, the turnover for this type of applications is expected to increase $2.9x10^9$ USD, an industry that will probably be led by U.S., Germany, Japan and China [4]. For this same period, forecasts indicate that the production of titanium dioxide nanoparticles will reach the 10^4 annual tons [5].

A novel continuous photocatalytic system based on a porous mesh coated with a photocatalytic paint incorporating 9 wt.% of TiO_2 was tested. Two wire mesh materials were tested, plastic and stainless steel. Photoinactivation assays were performed with cell suspensions of a Gram-negative bacterial strain (*Escherichia coli* DSM 1103) with an initial density of 1×10^6 cells mL^{-1} under at flow rate of 2 $mL \cdot s^{-1}$ for 40 min.

Viability losses of 54.1 % and 39.4 % were obtained for the 2 x 2 mm^2 and 3 x 3 mm^2 stainless steel meshes, respectively, after 40 min irradiation. The effect of the surface area is important because of the amount of TiO_2 available determines the formation of hydroxyl and superoxide radicals needed for inactivating bacteria. Viability loss of 89.4 % was obtained for 80 min irradiation. This finding also may due to a possibility that there is a linear relationship between irradiation time and inactivation. The results indicate an efficient combination of procedure and photocatalytic continuous system executing in the inactivation of the *E.coli* bacteria. The results of this study suggest that the developed tecnology could be improved on the future.

Keywords: photocatalysis, water disinfection.

Declaration

Declare, under oath, that this work is original and that all non-original contributions were properly referenced with source identification.

_____

Sign and date

Table of Contents

List of Figures

List of Tables

1- Introduction

1.1 - Background and Scope

One of the priceless and not replaceable natural resource on earth is the water. Presently, water resources contamination is one of the most pressing concerns. In 2002, the World Health Organization (WHO) reported than one out of six people, representing 17% of the global population, lacked access to safe drinking water. More so, water contamination has been causing the death of thousands of people every year since it enhances the dissemination of diseases [6, 7]. It is also estimated that around 4500 children die every day due to the same issue.

In the 20^{th} century alone, the world population more than tripled. Furthermore, it is expected to increase by another 40-50 % within the next 50 years. This intensive growth raises two relevant issues. First, it will increase the water demand, exacerbating the scarcity of clean water and second it will increase the number of deaths related to contamination of water resources [1].

Water contamination can be either of chemical or biological nature, and both pose important risks to the public health. On the one hand, chemical contamination has been a relevant concern over the course of the last decades. Our awareness of this problem has been continuously improved by the development of superior analytical technologies and by the increasing numbers of toxicological studies, correlating contamination with specific illnesses such as cancer [8].

In order to overcome this type of contamination the European Union created a new regulation called REACH (Registration, Evaluation, Authorization and Restriction of Chemical substances), which strictly regulates the use of chemical substances. This regulation protects both the environment and the public health and, at the same time, guaranties the competitiveness of the EU chemical industry [9].

On the other hand, biological contamination of the water resources is defined by the emergence and spreading of pathological microorganisms in water. Presently, this is leading to an increased number of new infections each year. According to statistics provided by the United States healthcare, every year approximately 2 million new cases of infections are reported, causing a total of 100,000 deaths (Fig. 1). In the European

Union (EU), 320,000 new cases are reported annually, but the real value is estimated to be much higher [10]. Ultimately, this has led to increased expenses for the governments and has increased the search for low-cost and highly effective methods to control this type of contamination [7, 11-14].

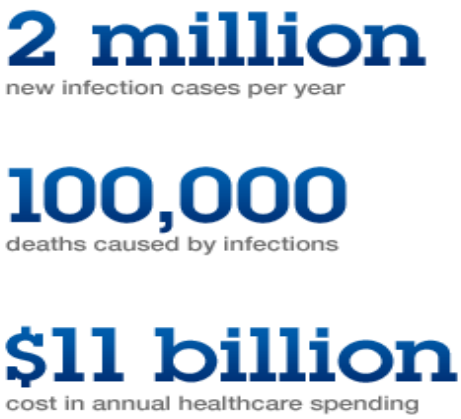

Figure 1. Statistical information from the United States healthcare [14]

In order to contain the negative effects of water contamination some disinfection methods were developed in the last decades. The most popular ones include ozone exposure, irradiation with UV light, and chlorination. These methods rely on the use of powerful chemical oxidising agents such as chlorine, chlorine dioxide or ozone; however, they have relatively short periods of activity [2, 3]. Hence this raised the need to explore unconventional technologies for water treatment.

In this context, Advanced Oxidation Processes (AOPs) emerged as a viable and efficient alternative. Within the diverse list of processes, photocatalysis mediated by Titanium dioxide (TiO_2) proved to be an important method for water-disinfection due to its bactericidal activity [1, 15, 16].

In this study it was developed a novel water-disinfection treatment using a continuous photocatalytic system. One remarkable advantage of this system is employing a paint coat containing TiO_2 immobilized, instead of using hazardous oxidizing agents. This study is divided in four different tasks. These tasks seek the improvement of the photocatalytic system, discovering the critical variables to attain high efficiency of photoinactivation activity. This study started with the assembly and set up of the continuous photocatalytic system. The second task focused on evaluating different mesh support materials (i.e. inert, irregular area and possible to sterilize) and also the effect

of mesh porous size. The third task focused on the incorporation of 9 wt. % of TiO_2 in the paint effectively. And, finally, the fourth task focused on the evaluation of several experimental parameters, such as flow rate and irradiation time in order to discover the optimal operating parameters. The results obtained suggest that the continuous photocatalytic system developed has potential to disinfect water.

Principles of Photocatalysis

Fujishima and Honda (1972) were the firsts to realize the potential of TiO_2 as a photocatalyst. By using TiO_2 photoanode in combination with a platinum counter electrode soaked in an electrolyte aqueous solution, they were able to achieve ultraviolet light-induced water cleavage [16]. This reaction is based and inspired on the natural process of photosynthesis, used by plants, algae, and cyanobacteria to harvest and convert light into electrochemical potential [17-19]. In this process, the chlorophyll absorbs the photons and losses one electron, which immediately initiates the flow of electrons down a transport chain and ultimately leads to the production of energy. Similarly, TiO_2 absorbs the photons provided by ultraviolent radiation, allowing the migration of the electron in the valence band to the conduction band; ultimately, this lead to the cleavage of the water molecule.

The use of nanoparticules in water treatment technologies has been increasing in latest years. Between 2008 and 2015, the turnover for this type of applications is expected to increase $2.9x10^9$ USD, an industry that will probably be lead by U.S., Germany, Japan and China [4]. For this same period, forecasts indicate that the production of titanium dioxide nanoparticles will reach the 10^4 annual tons [5].

In particular, photocatalysis with TiO_2 has been applied to a broad range of research areas, especially environmental and energy-related fields [19-23]. It is a heterogeneous process since it occurs both in liquid (water) and solid phases (photocatalyst nanoparticles) and presents the advantage of being easily monitored using simple methods such as the decomposition of phenol or methylene blue, etc [11, 15].

TiO_2 induces a simple photocatalytic reaction when it is impacted by energy photons with a wavelength of 386 nm. If this reaction happens in the presence of oxygen it will produce highly reactive free radicals like hydroxyl (OH·) and superoxide ($O_2\cdot^-$). Afterwards, the reactive radicals carry out the disintegration of organic particles and microorganisms contained in the water, without generating toxic by-products [6].

Disinfection with TiO_2 has been a widely studied process since the breakthrough work of Matsunaga, Tomoda [24]. These authors were able to achieve 99 % inactivation of a bacterial cell suspension using a photo-reactor containing TiO_2. Nevertheless, the mechanism behind the photo-inactivation process is still not fully understood.

1.2 - Aim and Outline

General objective:

1- Design of a novel continuous photocatalytic system based on a porous support mesh coated with a photocatalytic paint incorporating 9 wt.% of TiO_2 to photoinactivate microorganisms in an aqueous system.

Specifics objectives:

1- Design and assemble a continuous photocatalytic system

2- Evaluate the efficiency of the three-dimensional structure of TiO_2 in aqueous system

3- Evaluate different mesh support materials

4- Evaluate experimental parameters such as irradiation time and flow rate

Outline: In this dissertation experimental and theoretical aspects of photocatalysis are covered. It includes in chapter 1 the introduction, in which the justification and background of the study project are presented. In chapter 2 includes the state of art on the scientific advances of photocatalysis, the use of TiO_2 as photocatalyst in photoinactivation of microorganisms. In chapter 3 the technical description of the experimental work is given, which includes the purpose of the novel continuous photocatalytic system, the photocatalytic paint coating and the photoinactivation assays.

Chapter 4, includes the main results obtained. In the end, the conclusions of the work are presented, as well as future scopes and final assessment of the work.

1.3 - Contributions

Innovative ideas: 1- Use of TiO_2 immobilized in three-dimensional position.

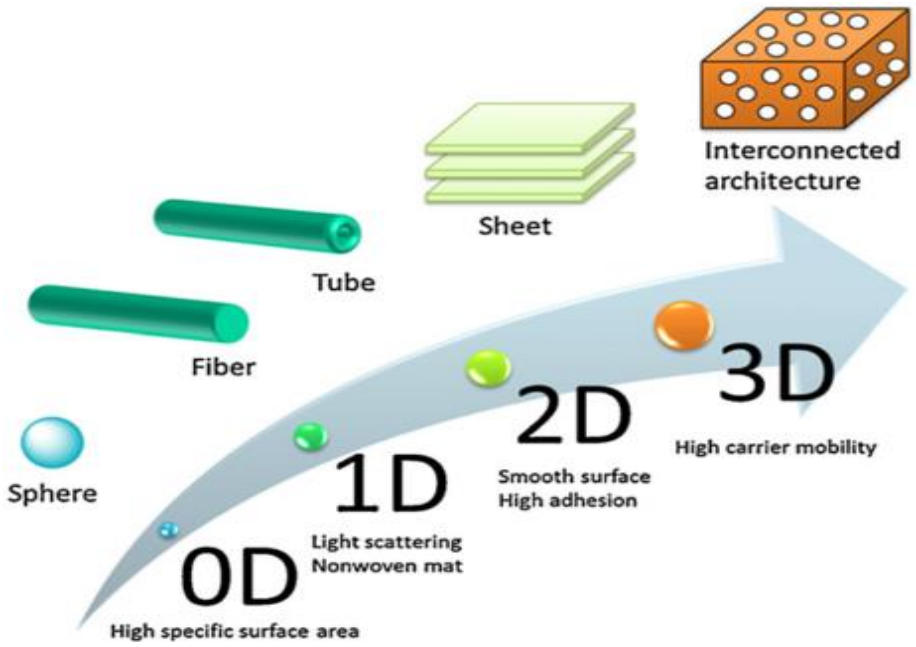

Figure 2. Schematic illustration of structural dimensionality of materials with expected properties [25].

Photocatalytic activity has been evaluated using different structures such as spheres, fibers, tubes and sheets (Fig 2). Yet, none of these structures achieved high efficiency in aqueous medium. This study innovates by employing a three dimensional structure supported in a paint coat. Meanwhile, it also aims to overcome three important aspects. Firstly, maximize the absorption of light. Secondly, maximize the interfacial area with the bacteria. Thirdly, allow the liquid phase to have more contact with the free radicals produced.

2- A novel continuous photocatalytic system was developed to photoinactivate microorganisms in an closed aqueous system.

2- State of Art

2.1 Photocatalysis

A chemical reaction mediated by a solid material in the presence of light is by definition a photocatalytic process. In reactions of this nature the photocatalyst remains unchanged throughout the entire process and only play an indirect role in this process [15].

Firstly the catalyst absorbs photons and if these photons have a sufficient amount of energy they will excite electrons of the valence band. In this case electrons will jump the "band gap" and migrate to the conduction band [20, 28]. Hereupon the migration of the photon leaves a hole in the valence band:

$$\text{photocatalyst} + h\nu \longrightarrow e_{cb}^{-} + h_{vb}^{+} \qquad (2.1)$$

The photocatalytic process occurs on the surface of the catalyst and, therefore, its efficiency is highly influenced by the intensity of the radiation, spectrum of the light source, concentration of both photocatalyst and pollutant and temperature [26].

Photocatalysis can be either homogeneous or heterogeneous, depending if the catalyst is or is not in the same phase. Heterogeneous processes occur under two situations, when the catalyst particles are suspended in contaminated water and when the catalyst is immobilized on the surface of various inert substrates [4].

Some advantages of the hetereogeneous photocatalysis, as efficient oxidizer of organic compounds, are: (1) The possibility of being activated by solar radiation could result in low energy costs; (2) It may not need post-treatment since the organic pollutants may be mineralized into non-toxic by products such as H_2O, CO_2, and mineral acids [27].

2.2 Photocatalysis mechanism

As shown in figure 2, the photocatalytic reaction begins as soon as the irradiation (*hv*) reaches the catalyst.

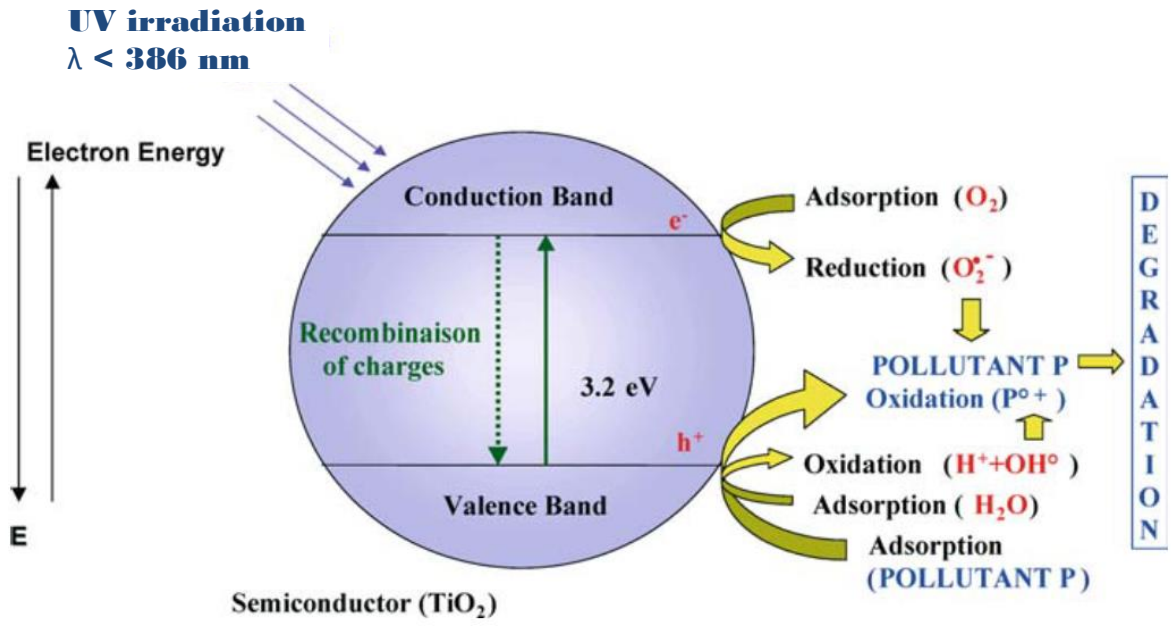

Figure 3. Energy band diagram illustrating the formation of photogenerated charge carriers (hole [h^+] and electron [e^-]) upon absorption of ultraviolet (UV) light producing the free radicals (superoxide and hidroxyl) participating in the photoinactivation of E.coli on TiO_2 surface. Modified from [26].

The photogenerated holes in the valence band diffuse to the TiO_2 surface and react with adsorbed water molecules, forming hydroxyl radical (OH•) and hydrogen ion (H^+) [11, 25, 27] (Fig. 4),as shown in the equation 2.2:

$$h_{vb}^{+} + H_2O_{ads} \rightarrow OH^{\bullet}_{ads} + H^{+} \qquad (2.2)$$

Both the photogenerated holes and the hydroxyl radicals participate in the oxidation of the nearby organic molecules. Meanwhile, electrons in the conduction band typically participate in reduction processes. This process comprises the reaction with the molecular oxygen in air and leads to the production of superoxide radical ($O_2^{\bullet -}$) [25, 27] (Fig 4), as shown in the equation 2.3:

$$e_{cb}^{-} + O_{2ads} \rightarrow O_2\cdot^{-} \quad (2.3)$$

The free radicals, hydroxyl radical (OH•) and superoxide anion radical ($O_2\cdot^{-}$) have been proposed hypothetically since the early stage of research on photocatalysis involving TiO_2 as photocatalyst. Such active free radicals may have a relatively short lifetime due to their natural stability, and therefore *in situ* detection is not easy [15].

2.3 TiO_2 as a photocatalyst

Titanium dioxide can exist in three distinct crystallographic forms: anatase, brookite, and rutile. Brookite is a naturally occuring phase, and is extremely difficult to synthesize. Anatase and rutile also occur naturally, but can be synthesized easily in the laboratory [28]. Anatase and rutile are the most popular catalysts used (Fig. 3), the crystallographic structures are shown in Fig 4. These photocatalysts absorbs light to achieve a higher energy state [15]. Anatase is able to absorb only ultraviolet light, at a wavelength shorter than ca. 386 nm (corresponding to 3.2 eV). Many authors can increase this absortion into visible light, usually doping a metal or nonmetal atom to the TiO_2, to facilitate the application of this photocatalyst using indoor light.

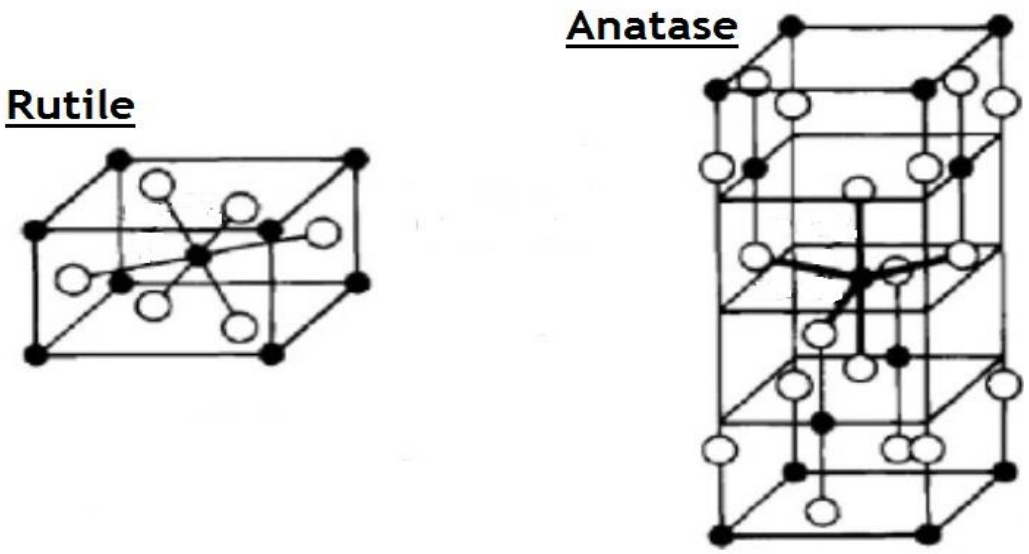

Figure 4. Structure of rutile and anatase TiO_2. Modified from[29]

TiO_2 photocatalyst has been the most widely studied and used in many applications because of its strong oxidizing abilities, for the decomposition of organic pollutants,

superhydrophilicity, chemical stability, long durability, nontoxicity, low cost, and transparency to visible light [16, 18, 25, 30-33]

The most recognized producers of TiO_2 are Evonik (Degussa), Millenium Inorganic Chemicals, Kronos, Sachtleben, Tayca and Kemira [34, 35].

2.3.1 Titanium Dioxide Modifications

Nowadays, the extension of TiO_2 applicability as photocatalyst is being investigated. To achieve this goal many studies are making efforts to get an increased absorption spectrum from UV into the visible light. For this reason, three different stages are presented to classified the modifications generations that TiO_2 has experienced [30].

First Generation: Pure TiO_2

When the TiO_2 particles decrease, the amount of atoms located at the surface increases, enhancing the photocatalytic activity. The band gap energy exclusively increases when nanoparticle size decrease, (this phenomena occurs below certain nanoparticle diameter: quantum confinement), enhancing the redox potential of the valence band holes and the conduction band electrons, carrying out photoredox reactions. One inconvenience of TiO_2 nanoparticles is that they are able to use a small percentage of sunlight for photocatalysis. Even that the majority of the solar irradiation reaching the Earth's surface is visible light (VL) and only 4 % is UV. In experimental level, exists an optimal size for specific photocatalytic reaction [29].

There were previous studies investigating the photocatalytic activity of TiO_2 nanoparticles in different reactions, e.g, hydrogenation reactions of CH_3CCH with H_2O, the decomposition of chloroform, the decomposition of 2-propanol and nanotubes treated with H_2SO_4 solutions to degradate acid orange [29].

Second Generation: Metal-Doped TiO_2

Metal-doped TiO_2 are well-known nanomaterials for being used on the degradation of several organic pollutants, i.e., under visible light irradiation [36].

There were previous studies investigating the photocatalytic activity of metal-doped TiO_2 in different reactions, e.g., 21 transition metal elements on the oxidation of $CHCl_3$ and the reduction of CCl_4, Sn^{4+} ion-doped TiO_2 prepared by the plasma-enhanced

Chemical Vapor Deposition method for photodegradation of phenol and Fe-doped in the treatment of paper-making wastewater and disinfection of *E.coli [29].*

Third Generation: Nonmetal-Doped TiO_2

Nonmetal-doped TiO_2 are well-used materials for their visible light photocatalytic activities. Nonmetal-doped TiO_2 demonstrated to improve their photocatalytic activity compared with pure TiO_2 nanomaterials [29].

There were previous studies investigating the photocatalytic activity of nonmetal-doped TiO_2 in different reactions, e.g., N-doped TiO_2 used for the decomposition of methylene blue, S-doped TiO_2 tested under both visible and UV region and C-doped TiO_2 used for the decomposition of methylene blue and isopropanal [29].

2.3.2 Titanium Dioxide Applications

Over the course of the last decades photocatalytic systems have been developed for a wide range of applications (Fig. 4). TiO_2-photocatalysis is mainly applied in solar and photoelectrochemical cells, environmental and energy field. Another relevant application is the photobleaching of organic or microbial pollutants both in liquid and gas phases [26].

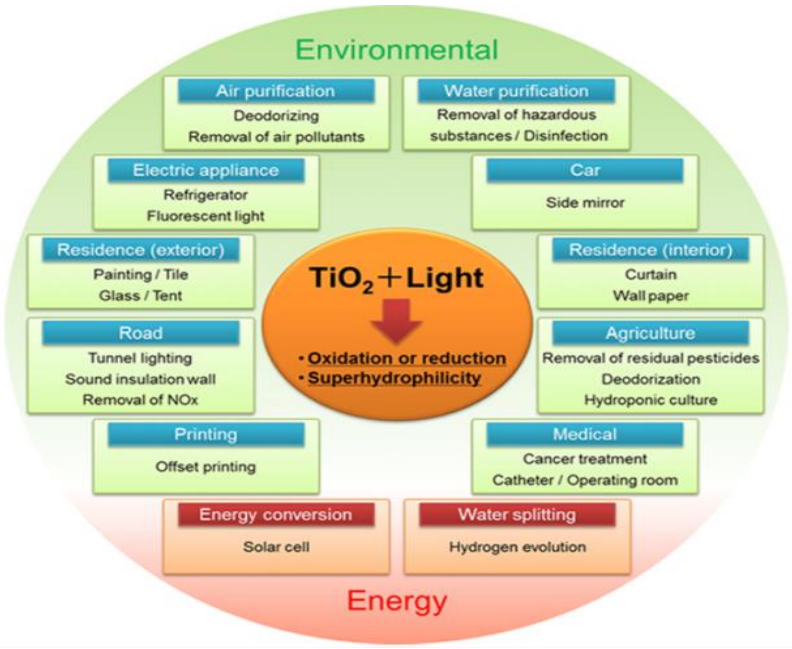

Figure 5. Applications of TiO_2 photocatalysis [25].

2.4 Escherichia coli

Escherichia coli belongs to the class of *Gammaproteobacteria* and to the order of the *Enterobacteriales*. They are rod-shape, nonspore-forming, Gram-negative bacteria and an inhabitant of the terminal small and large intestine of mammals. To this day *E.coli* is one the best well-studied and characterized microorganisms [37].

These bacteria are able to replicate outside the intestine. However, they can survive in soil and water up to 12 weeks [38]. Its presence in environmental samples is an indicator of fecal contamination. Because of that *E.coli* is an ideal biological indicator and model organism for many studies. In this study, strain DSM 1103 [39], was used to assess the efficiency of TiO_2/UV-A photoinactivation process in a continuous system.

2.5 Photoinactivation mechanism

The biocide effect produced by TiO_2 when combined with UV-A irradiation in a rich oxygen atmosphere has been attributed to the generation of very active free radical species, also referred to as reactive oxygen species (ROS), on the catalyst surface [19, 24, 40, 41]. The main ROS involved in this process are the hydroxyl ($OH^{\bullet}$) and superoxide radicals ($O_2^{\bullet -}$), previously shown in equations 2.2 and 2.3.

Various studies on models of microbial destruction through photoinactivation suggest that the initial target of the photocatalytic process is the bacterial cell wall [24, 42-44]. After damaging the outer membrane, these free radicals, attack the phospholipids of the cytoplasmatic membrane (Fig. 5) through a process designated as lipid peroxidation.

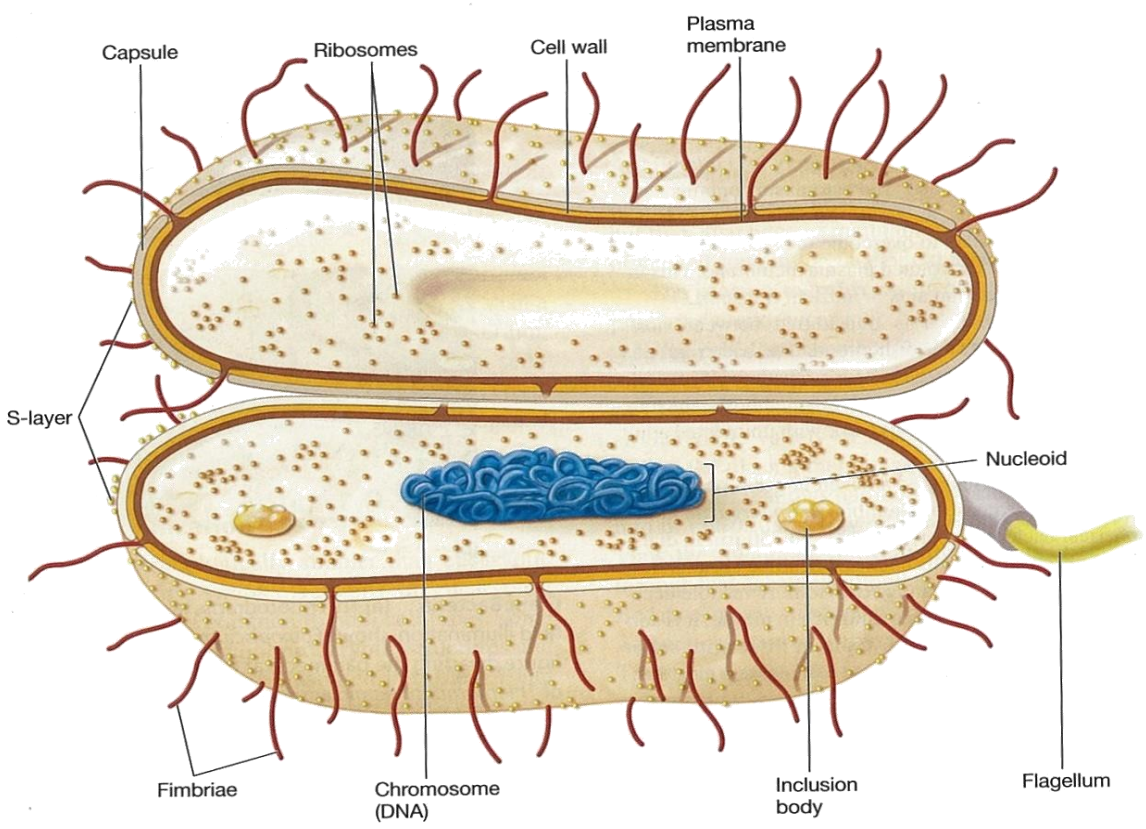

Figure 6. Schematic representation of a prokaryotic cell [45].

The oxidation of the lipids leads to the formation alcoxil and peroxil radicals [46] and, ultimately to the loss of membrane permeability [44, 47]. This loss will promote two parallel processes (Fig. 6). On the one hand it will cause the release of ions K^+ and macromolecules such as proteins and nucleic acids [48], leading to cell disruption. On the other hand, it will cause the depletion of coenzyme A through dimerization, with consequent inhibition of the respiration process [49]. Both these phenomena cause loss of cell viability and, ultimately, lead to cell death, which suggests that photoinactivation is an adequate method to eliminate microbial contamination [47]. This process proceeds even after the separation of the cells from the TiO_2 surface [42].

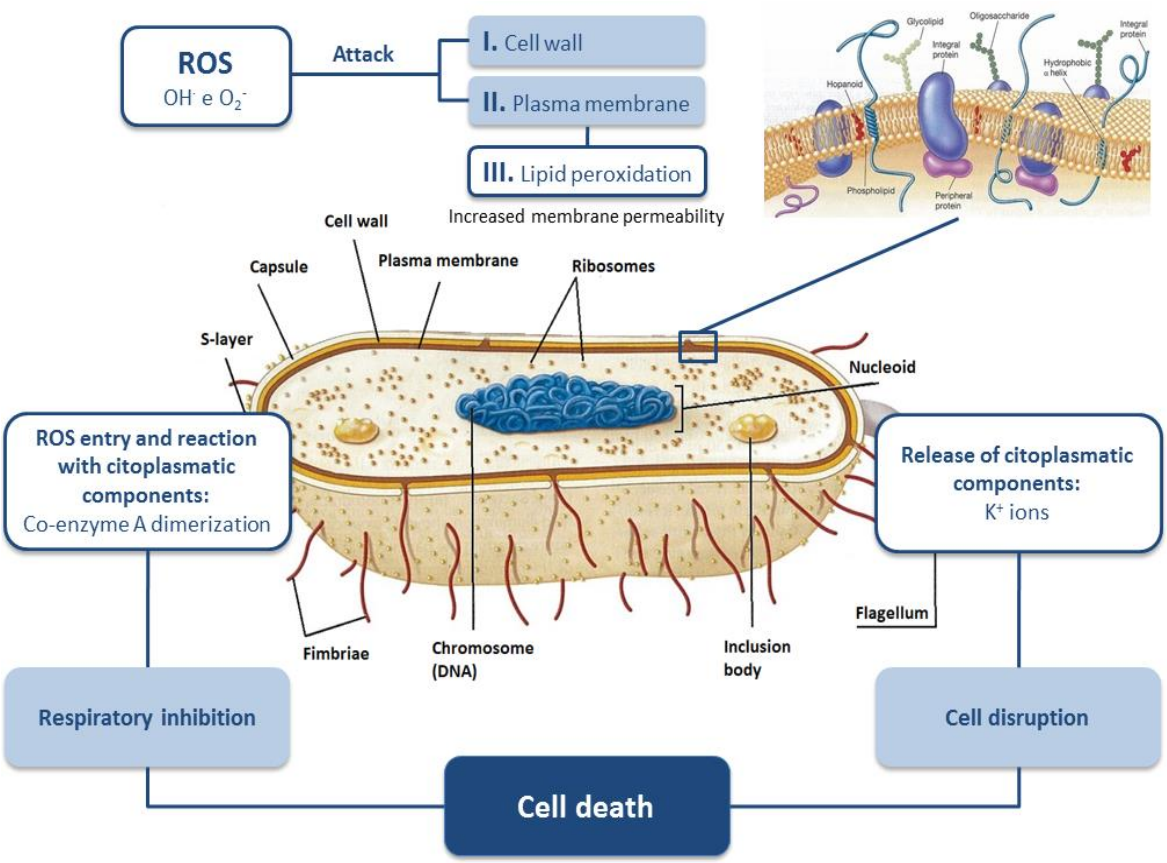

Figure 7. Suggested mechanism for cell death throught photoinactivation with TiO_2. Modified from [45].

3- Technical description

The technical description section its divided in three parts: the design of a novel continuous photocatalytic system, the composition of the photocatalytic paint and the *Escherichia coli* photoinactivation procedure.

3.1 Design of a novel continuous photocatalytic system

The novel continuous photocatalytic system, shown in figures 5 and 6, is based on a porous mesh materials coated with a photocatalytic paint incorporating 9 wt.% (wet basis) of TiO_2 (Aeroxide version of P25, Evonik Industries, Germany).

Figure 8. Experimental continuous photocatalytic system

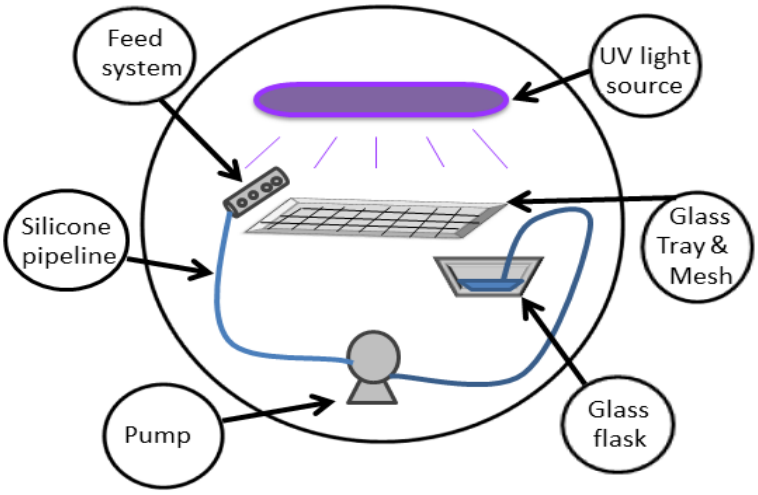

Figure 9. Scheme of the continuous photocatalytic system based on a porous grid coated with a photocatalytic paint incorporating 9 wt.% of TiO_2 to photoinactivate the bacteria E. coli DSM 1103

Two wire mesh materials were tested, plastic and stainless steel. The wire mesh had measurements of 6 cm width x 16 cm length equivalent size of the two black-light-blue bulbs together. The porous size used were 2 x 2 mm^2 and 3 x 3 mm^2 for the stainless steel mesh, and 2 x 2 mm^2 for the plastic mesh. The selection of this dimension was on purpose to use the available surface area where the photocatalyst was available. It was necessary to employ a mesh support, designated glass tray, where mesh fit inside. Thus, the dimensions of the glass tray were similar as the wire mesh 6 cm width x 16 cm length, with the only exeption that the wire mesh was cut for 1 or 2 mm less in order to fit. A cell suspension, 100 mL with 1x 10^6 cells·mL^{-1} of the bacteria *E. coli*, was homogenized by agitation of 600 rpm (Falc F 30, Italy) inside a glass flask, in order to avoid the presence of biofilms and also to guaranteed a constant cell concentration in the glass flask, specially when the samples were taken.

The recirculation of the cell suspension was done using a peristaltic pump (Watson Marlow 323, United Kingdom) with a flow rate of 2 mL·s^{-1}. This flow rate was established in order to guarantee the highest posibility contact between the pollutant (bacteria) and the photocatalytic mesh coated to enter in contact with the bacteria contained in the water. Additionally, two different flow rates, 1 and 4 mL·s^{-1} were used to determined the relationship between the flow rate, residence time and photoinactivation. The number of cycles of the contaminated water using different flow rates were calculated,

they are shown in appendix 5. The residence time was also calculated to represent the small difference between the values from the flow rates, not even 1 order. For this case of study, close and continuous system is more representative to investigate and justify in cycles terms, see appendix 6.

A feed system was made with stainless steel material, 9 cm length x 4 mm internal diameter and 6 uniforms holes located one milimeter of distance in between each one (the design in solidworks® is shown in appendix 1), connected with a silicone pipeline with 4 mm external diameter x 1 m length, containing 6 uniforms holes, each hole is located one milimeter of distance in between.

The uniformity of the holes was designed to guarantee an homogenized initial out flow. It is important to mention that the feed system and the glass tray were interconnected in a plastic piece. The plastic piece was created to expedite the assembly of both feed system and glass tray. A light source is described in the next item 3.1.1, however was installed 90° to the glass tray, to promote the highest irradiation impact possible uppon the available surface area.

3.1.1 Light source and apparatus

The ultraviolet (UV-A) lamp had a high intensity wavelength with emission at 365 nm. It contained two 6 W black-light-blue bulbs (VL-206-BLB. Vilbert Lourmat, France). It was measured its incident photon flux with a UV radiometer (HD 2102.2, Delta/OHM, Italy) and set up at 10 W/m^{-2} for the photoinactivation assays according to ISO/DIS 27447 (2009) and at 30 W/m^{-2} for pre-activation of the coated mesh.

3.2 Photocatalytic paint

The photocatalyst used was the Aeroxide version of TiO_2 P25 (Evonik Industries, Germany), which crystallinity composition is 80:20 anatase:rutile and specific area of 50 $m^2\ g^{-1}$. The paint followed a modification of vinyl matt formulation described elsewhere since it did not include thickeners [50]. Briefly, the base paint was aqueous and contained inorganic components in powder form, extenders, and organic components which are the binder (resin), dispersing agents, the coalescent, additives and the polymer extender slurry [51]. No biocides were added, and were replaced by water.

All the materials were provided by CIN S.A.

3.3 Photoinactivation procedure

The following procedures were under the ISO 27447:2009 known as "*Test method for antibacterial activity of semiconducting photocatalytic materials*" with some modifications included.

3.3.1 Microorganism and culture medium used

The model microorganism used in the photoinactivation assays in aqueous system was a Gram-negative bacterial strain *E. coli* DSM 1103, as cell suspension. More details of the cell suspension are given in 3.3.2 section.

The culture medium used to grow this bacteria was the Plate Count Agar (PCA, LiofilmChem, Italy), which is a growth medium that allows the development of different types of heterotrophic organs like bacteria and yeast. The composition is shown in appendix 2. Cultures were grown at 30 ºC, overnight (~20 h).

3.3.2 Preparation of Cell suspension

After incubation, the biomass grown on PCA plates was carefully observed to confirm the purity of the culture, i.e., presence of colonies of identical morphology. In addition, a Gram coloration assay was performed to assure that all cells were identical rod-shaped and with red colour (coming from the safranin pigment), which is indicative of the presence of Gram-negative bacteria.

A cell suspension with a initial concentration of $1x10^8$ cells mL^{-1} was prepared in a test-tube containing 9 mL of sterile saline solution [0.85 % NaCl (w/v)], using a calibration curve of optical density values at 610 nm vrs CFU (colony forming unit) / mL for the strain *E. coli* DSM 1103:

$$CFU/\,mL = 1x10^9\ DO\ (610\ nm) \qquad (3.1)$$

Two mililiters of this suspension was mixed with 18 mL of sterile saline solution (10 x dilution). Then, 10 mL from the new suspension was mixed with 90 mL of sterile saline solution (10 x dilution) contained in the glass recipient, $1x10^6$ cells·mL^{-1} as recommended. This procedure follows the ISO 27447.

3.3.3 Preparation of the painted meshes

The plastic and stainless steel mesh materials were painted using a paintbrush and exposed to environmental conditions for approximately 24 h to dry. After, they were sterilized in an autoclave for 30 min at 121°C. Finally the pre – activation of the photocatalytic paint coat was performed by exposure to 30 $W \cdot m^{-2}$ UV-lighthing irradiation, as shown in shown in figure 7.

Figure 10. Pre – activation procedure before and during the process.

3.3.4 Photoinactivation Assay

A modification of ISO 27447 [52] was used to assess the *E.coli* photoinactivation using the novel continuous photocatalytic system designed.

A set of assays were performed to compare the photoinactivation accomplished with P25 immobilized in a three-dimensional structure, within photocatalytic paint. Once the final cell suspension was prepared, it recirculated in the entire system and within the glass flask was homogenizing for approximately 30 min, both were set up simultaneously, as stabilization process. Once the stabilization ensured that the system was working suitably, the photoinactivation assay started to carry out.

At the initial (t_0) and final instant (t_f), 1 ml sample collected from the glass flask was transfered into a test tube containing 9 mL of sterile saline solution. The resulting cell suspension was serially diluted in sterile saline solution, and aliquots of 100 µL were spread on PCA, as described in Koch [53].

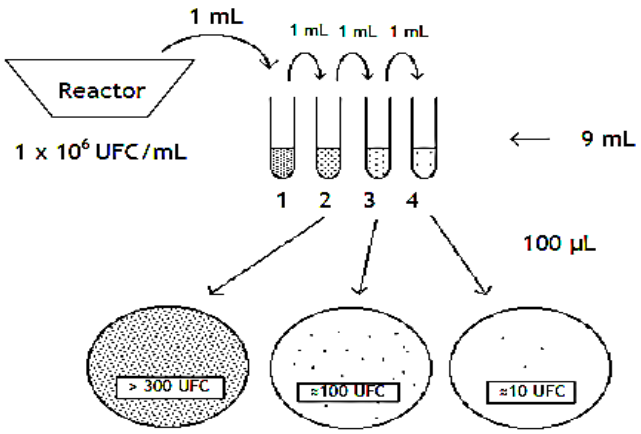

Figure 11. Scheme of the seriall dilution and spread method

After incubation at 30°C for 24 h, the viable cells were enumerated in cultures containing 30-300 CFU.

The percentage of photoinactivation (equivalent to viability loss) and log reduction was determined as shown in (equation 2) and (equation 3), respectively:

$$\text{Viability loss (\%)} = [(M_i - M_f) / Mi] \times 100 \quad (3.2)$$

$$\text{Log reduction} = \log_{10} (M_i - M_f) \quad (3.3)$$

Where M_i and M_f are the initial and final *E. coli* viable counts, respectively.

The antimicrobial effect of the photocatalyst was calculated by the difference between the initial (t_0) and final (t_f) number of viable cells with the equation 5. The reduction rate (inactivation) of viable cells in the final contact time between the suspension and the photocatalyst was calculated according to the equation 7 and 8, respectively.

$$\text{N° CFU} = (\text{n° CFU} \times D + \text{CFU duplicate} \times D) / 2 \quad (3.4)$$

Where D its the dilution factor.

$$\text{\% reduction} = [(\text{CFU / mL initial} - \text{CFU / mL final}) / (\text{CFU / mL initial})] * 100 \quad (3.5)$$

3.3.5 Pure TiO_2

Pure TiO_2, equivalent to maximum efficiency assay was performed in the absence of any coated mesh on the glass tray. The amount of the photocatalyst (appendix 3), equivalent to the weight contained in every coated mesh, was spread uniformly along the glass tray surface. The remaining experimental conditions were equivalent to the other assays.

3.3.6 Controls

Controls assays in the dark and under UV-A irradiation were performed to assess the influence of the experimental conditions and of the irradiation on cell inactivation, respectively. All the assays were performed in duplicate, inside a clean chamber.

3.3.7 Statistical analyses

One-way ANOVA´s tests (R by R Foundation, V. 2.14.1) and Student´s t-test (MS Excel® 2010) were used to assess statistically significant differences ($p < 0.05$) among the percentage of photoinactivation of the assays performed.

The statistical analysis made in the present study is detail shown in appendix 8.

4- Results and Discussion

4.1 Continuous photocatalytic system

The first part of the experimental work aimed at designing the photocatalytic system. Thus, the system was assembled and technical inconveniences were solved.

Firstly, the mesh was installed in a glass tray. After, it was chosen a glass tray because the walls hampered water leakage and, thus, it was possible to get a water layer over the mesh, guaranteeing the highest possibility contact between the TiO_2 and the bacteria over the assays. Secondly, a feed system with silicone was designed, but the holes were not uniform implicating a bad flow out. Then, it was decided to make another feed system using stainless steel with six uniform holes to facilitate the distribution of the fluid.

Thirdly, a plastic support that would hold the glass tray and the feed system simultaneously was designed, with a similar altitude of the glass flask. The assembly of the feed system and glass tray became easier to arrange and, consequently, the photoinactivation assay became faster.

The first mesh material tested was sacking. After painted, the sacking did not stay stretched, but constricted. Being constricted made it impossible to maintain the sacking in an adequate position on the glass tray, turning infeasible to run adequately the photoinactivation assay. Being constricted painted sacking influenced the flow pattern, since preferential paths occurred when the fluid was passing through it. For these reasons the sacking was discarded.

This study aimed at designing a new water disinfection method. Thus, the influence of experimental parameters (contact area, surface area, flow rate, amount of photocatalyst and irradiation time), on the photoinactivation activity of the system under a constant radiation intensity was assessed.

4.2 Viability loss and log reduction of various configurations of the continuous photocatalytic system

In this section it is presented the results of inactivation of *E. coli* DSM 1103 obtained in controls and assays.

4.2.1 Results of dark controls

The viability loss in dark obtained for the pure TiO_2, was approximately 4 % (Table 1). These results indicate that neither the photocatalyst nor the experimental configuration had prejudicial effects on the microorganism, confirming previous studies [24, 54-56]. This finding proves the ability of the *E.coli* DSM 1103 to survive on recirculating aqueous suspension during the assay period (40 min).

4.2.2 Results of UV-A irradiation controls

The maximum contribution of UV control was found for the 80 min irradiation time, about 35 % (Table 2). Such a result was expected because there is a directly relationship between the irradiation time and the mutagenic effect of UV-A [57].

The pure TiO_2 assays were performed by spreading the catalyst uniformly upon the glass tray. Consequently, the absence of a mesh permitted the unimpeded irradiation of the tray and, most likely, the increased production of free radicals. Due to these conditions the assay resulted in a viability loss of 29 % (Table 1), the second highest value observed in this study.

For the assays containing the coated mesh on the surface of the glass tray, as it is showed on tables 1 and 2, the values of UV-A irradiation were significantly lower, ranging between 8 % to 18 % ($p < 0.05$). These lower values may be due to a decrease of UV irradiation impact upon the layer of water passing below the coated mesh, i.e., due to the intermittent UV-A irradiation impact under the bacteria.

Table 1. E. coli viability loss (%) after 40 min of UV-A irradiation at 10 $W \cdot m^{-2}$ and in dark conditions in continuous photocatalytic system at a flow rate of 2 $mL \cdot s^{-1}$.

	% viability loss		
Material	TiO_2 (P25) photocatalysis	UV light only	TiO_2 (P25) in dark conditions
Pure TiO_2	99.8 ± 0.1 c, C	29.1* ± 2.0 B	3.9 ± 4.8 A
1 - Stainless steel 2 x 2 mm^2	54.1 ± 4.1 b, B	8.1 ± 4.0 A	0.0 ± 0.0 A
2 - Stainless steel 2 x 2 mm^2	53.2 ± 4.0 b, B	8.1 ± 4.0 A	0.0 ± 0.0 A
Stainless steel 3 x 3 mm^2	39.4 ± 3.3 a, C	18.1 ± 11.0 B	0.0 ± 0.0 A
Plastic 2 x 2 mm^2	38.4 ± 0.3 a	---	---

Values are means ± standard deviation (n=3). Within a column, lower-case letters indicated significant differences as determined by the Tukey test at $p < 0.05$. Within a row, significant differences between TiO_2 (P25) photocatalysis, UV light only and TiO_2 (P25) in dark conditions assays on the basis of the two-sample t-test at $p < 0.05$ are indicated by upper-case letter. Two viability loss assays were performed for the stainless steel (2 x 2 mm^2) material, with two months difference, the reproducibility is demonstrated that are not statistically different, as shown in table 1. * Assay without any mesh on the glass tray and any TiO_2.

4.2.3 Effect of materials

Viability losses of 54.1 % and 38.4 % were obtained for meshes with the same porosity (2 x 2 mm^2) of stainless steel and plastic, respectively. These values were very low when compared with the pure TiO_2 control (99.8 %). Such a difference indicates that painted mesh material should be further optimized.

4.2.4 Effect of porous size

Comparing the same support material with different porous size (stainless steel; 2 x 2 mm^2 and 3 x 3 mm^2), higher viability loss values were obtained for the lower porous size mesh support. This finding is reasonable as long as the smaller porous size means larger surface area and consequently higher photoinactivation activity.

In order to facilitate the comprehension of this scientific principle is illustrated (Fig. 11) the relationship of the pore size and the surface area. This system refers to a surface

process [26], so, it is possible to confirm that a smaller porous size implies a larger surface area involving a larger amount of TiO_2 available that determines the formation of superoxide and hydroxyl radicals necessary for inactivate the bacteria.

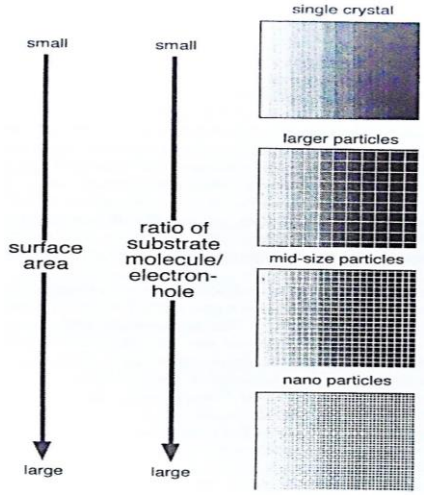

Figure 12. Schematic representation of the particle-porous size and surface area [16].

For the same porosity (2 x 2 mm^2), viability losses of 54.4 % and 38.4 % were obtained for meshes of stainless steel and plastic, respectively. The plastic mesh presented a thinner wire, reflecting in the amount of photocatalyst and the available surface area. The plastic was discarded; the next assays were performed with stainless steel.

4.2.5 Effect of irradiation time

The viability loss of stainless steel 2 x 2 mm^2 at two different irradiation times, 40 and 80 min, were 54.1 % and 89.4 % (Table 1 and 2), respectively, demonstrating that, as expected, viability loss was positively correlated with irradiation time. Considering energy consumption expenses, irradiation for 40 min would be advantageous. However, at these conditions, only half of the initial cell density is inactivated.

4.2.6 Effect of flow rate

The efficiency of photoinactivation process may be influenced by three related aspects: short lifetime of ROS, their unknown diffusion mechanism and kinetics and the time of effective contact between the cells and ROS. The free radicals diffusion determines their availability to react with the bacteria. Meanwhile, the flow rate determines the amount and frequency of contact between the bacteria and the reactant.

In this thesis it was observed a viability loss of 54.1 % for the 2 $mL \cdot s^{-1}$ assay (96 cycles, 40 min irradiation [Fig. 13]). While both the assays carried out with 1 $mL \cdot s^{-1}$ and 4 $mL \cdot s^{-1}$ presented lower values. The result for the low flow rate can be explained by a reduced number of impacts between the biomass and catalyst. And at the higher flow rate the period of contact between these two may be insufficient to cause the disruption of the cells.

Table 2. E. coli viability loss (%) after 40 min of UV-A irradiation at 10 $W \cdot m^{-2}$ and in dark conditions in continuous photocatalytic system at a flow rate of 1, 2 and 4 $mL \cdot s^{-1}$, employing the stainless steel of 2 x 2 mm^2. For 80 min of UV-A irradiation assay was used a flow rate of 2 $mL \cdot s^{-1}$.

	% viability loss		
Experimental parameter changeable	TiO_2 (P25) photocatalysis	UV light only	TiO_2 (P25) in dark conditions
1 $mL \cdot s^{-1}$	13.9 ± 5.1 a	---	---
2 $mL \cdot s^{-1}$	54.1 ± 4.1 c, B	8.1 ± 4.0 A	0.0 ± 0.0 A
4 $mL \cdot s^{-1}$	40.9 ± 2.4 b, A	13.4 ± 1.9 B	0.0 ± 0.0 C
80 min	89.4 ± 1.2 C	34.7 ± 2.2 B	0.0 ± 0.0 A

Values are means ± standard deviation (n=3). Within a column, lower-case letters indicated significant differences as determined by the Tukey test at $p < 0.05$. Significant differences between TiO_2 (P25) photocatalysis, UV light only and TiO_2 (P25) in dark conditions assays on the basis of the two-sample t-test at $p < 0.05$ are indicated by upper-case letter.

These results suggest that the optimal flow rate is near 2 mL·s-1, and that both higher and lower rates are unfavorable for the photoinactivation process in this system. Beyond the biochemical explanation for this phenomena, hydrodynamics problems should also be taken into account, since fluids dynamics are likely to change according to the velocity of its circulation.

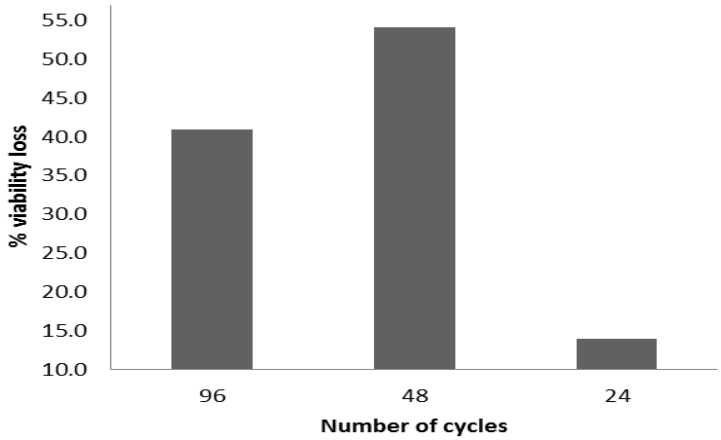

Figure 13. E. coli viability loss (%) in function of the number of cycles by the contaminated water along the photocatalytic system showing influence of the flow rate on viability loss. The calculations of number of cycles for 1, 2 and 4 mL·s-1 are shown in appendix 5.

4.2.7 Final assessment of results

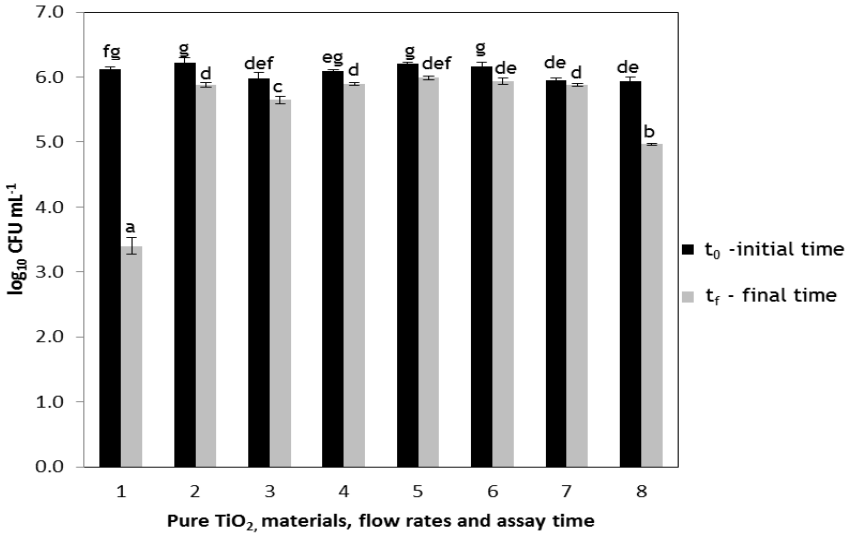

Figure 14. Photoinactivation ratio of E.coli DSM 1103 strain in different materials, flow rates and assays times with TiO_2 (P25, 9 wt.%) under ultra violet light (10 $W \cdot m^{-2}$). Results are mean values (n = 3) and the error bars represent the standard deviation. Significantly different values of log_{10} $CFU \cdot mL^{-1}$ are indicated by a, b, c, d, de, def, g, eg, and fg as determined by the Tukey test at $p < 0.05$. The numbers represented 1- Pure TiO_2, 2- 1. Stainless steel (2 x 2 mm^2), 3- 2. Stainless steel (2 x 2 mm^2), 4- Stainless steel (3 x 3 mm^2), 5- Plastic (2 x 2 mm^2), 6 – 4 $mL \cdot s^{-1}$, 7- 1 $mL \cdot s^{-1}$ and 8- 80 min.

Log differences for the pure TiO_2 and 80 min irradiation time (assay 1 and 8) were approximately 1 and 3, respectively (Fig. 14). The first finding confirms the high efficiency of TiO_2 on photokilling bacteria, as other studies had achieved [24, 44]. The second discovery suggests that this configuration has potential to disinfect water.

The remaining results, from 2 to 7 assay`s number, showed small significant difference ($p < 0.05$) between the initial and final time, approximately 1 log difference or even less, showing that the amount of cell death is no significant with the material, flow rate and assay time employed.

5- Conclusion, Outlook and Future Scopes

5.1 Achieved goals

The photocatalytic system developed in this study permitted to inactivate the test organism (*E. coli* DSM 1103).

The highest viability losses obtained were:

1- 99.8 % Pure TiO_2, 40 min and 2 $mL \cdot s^{-1}$.

2- 89.4 % 80 min assay time, 2 $mL \cdot s^{-1}$, stainless steel 2 x 2 mm^2.

3- 54.1 % stainless steel 2 x 2 mm^2, 40 min and 2 $mL \cdot s^{-1}$.

5.2 Limitations and future scopes

To this day, few related studies are available on the development of a closed aqueous photocatalytic system for the inactivation of microorganisms. For this reason, it was not possible to compare the results with other similar studies. Moreover, the experimental photocatalytic design could not be based on other studies and had to be made from scrath.

Regarding the future work, the following tasks are proposed:

Design of a new stainless steel photocatalytic system, integrating both the feed system and tray, enabling the sterilization of the entire structure and reducing the risk of external contamination.

Evaluate a new mesh material, extremely porous and with higher surface area.

Evaluate a new waterproof paint in order to prolong its durability in an aqueous system.

Determine the optimal flow rate in order to diminish the hydrodynamics problems. It is estimated to be near 2 $mL \cdot s^{-1}$.

Determine a cost-efficient irradiation time.

Evaluate another type of contaminant (bacteria), such as a Gram-positive strain.

Measure the production of $OH\cdot$ and $O_2\cdot^-$, to investigate the kinetics of the process and determine the efficiency of production of these free radicals.

Evaluate the morphological state of the coated mesh with scanning electron microscopy (SEM) or transmission electron microscopy (TEM), to determine the deterioration of the layer of paint caused by the photoinactivation assay. The properties of the immobilized TiO_2 could be altered if deterioration is observed.

Employ a different technique to paint the mesh, where the amount of photocatalyst can be controlled.

Calculate the ratio of number of bacteria and surface area necessary to achieve optimal efficiency; this may determine the other experimental parameters.

Propose a mathematical model to apply process dynamic and control to the system and find the optimal experimental conditions through simulation.

5.3 Final assessment

The purpose of this work is to serve as a starting point for the development of a larger scale system for pool's application.

The 3D configuration of the TiO_2/UV system applied in this thesis presented promising results for the inactivation of microrganisms.

The effect of the surface area is important because of the amount of TiO_2 available determines the formation of hydroxyl and superoxide radicals needed for inactivating bacteria.

The mesh support material is an important parameter as well; its available surface area and porosity determine the contribution to the photoinactivation activity.

The flow rate determines the shape and velocity of the water monolayer hydrodynamics.

There is no linear relationship between the flow rate and the photoinactivation activity of the system.

The best cost-benefit ratio of photoactivity efficiency was achieved with a 40 min assay time.

References

1. Teh, C.M. and A.R. Mohamed, *Roles of titanium dioxide and ion-doped titanium dioxide on photocatalytic degradation of organic pollutants (phenolic compounds and dyes) in aqueous solutions: A review*. Journal of Alloys and Compounds, 2011. **509**(5): p. 1648-1660.
2. Sohn, J., et al., *Disinfectant decay and disinfection by-products formation model development: chlorination and ozonation by-products*. Water Research, 2004. **38**(10): p. 2461-2478.
3. Meyer, B. and B. Cookson, *Does microbial resistance or adaptation to biocides create a hazard in infection prevention and control?* Journal of Hospital Infection, 2010. **76**(3): p. 200-205.
4. Ibhadon, A. and P. Fitzpatrick, *Heterogeneous Photocatalysis: Recent Advances and Applications*. Catalysts, 2013. **3**(1): p. 189-218.
5. Simkó, R.F.-M., *ITA Nanotrust Dossiers*, in *ITA Nanotrust Dossiers*. 2012, Eigenverlag/Self: Wien.
6. Chong, M.N., et al., *Recent developments in photocatalytic water treatment technology: A review*. Water Research, 2010. **44**(10): p. 2997-3027.
7. Organization, W.H., *The world health report 2002 - Reducing Risks, Promoting Healthy Life*. 2002, World Health Organization. p. 127-129.
8. Shy, C.M., *Chemical contamination of water supplies*. Environ Health Perspect, 1985. **62**: p. 399-406.
9. Agency, E.C. *REACH*. [cited 2013 25th of december]; Available from: http://echa.europa.eu/web/guest/regulations/reach.
10. Authority, E.F.S. *Food-borne zoonotic diseases*. 2013 [cited 2014 23th of january]; Available from: http://www.efsa.europa.eu/en/topics/topic/foodbornezoonoticdiseases.htm.
11. Ochiai, T., et al., *Development of a hybrid environmental purification unit by using of excimer VUV lamps with TiO2 coated titanium mesh filter*. Chemical Engineering Journal, 2013. **218**(0): p. 327-332.
12. Talon, D., *The role of the hospital environment in the epidemiology of multi-resistant bacteria*. Journal of Hospital Infection, 1999. **43**(1): p. 13-17.
13. Lemmen, S.W., et al., *Distribution of multi-resistant Gram-negative versus Gram-positive bacteria in the hospital inanimate environment*. Journal of Hospital Infection, 2004. **56**(3): p. 191-197.
14. Engler, A. *Amanda Engler talks about tiny infection-fighters*. 2013.
15. Ohtani, B., *Preparing Articles on Photocatalysis_Beyond the Illusions, Misconceptions, and Speculation*. Chemistry Letters, 2008. **37**(3): p. 217-229.
16. Kaneko, M. and I. Okura, *Photocatalysis: Science and Technology*, M.K.a.I. Okura, Editor. 2002, KODANSHA Springer: Japan. p. 1-5, 157.

17. Allen, J.F., et al., *A structural phylogenetic map for chloroplast photosynthesis.* Trends in Plant Science, 2011. **16**(12): p. 645-655.

18. Fujishima, A. *TiO2 Photocatalysis. Present Situation and Future Approach*. in *International Institute for Carbon-Neutral Energy Research* 2011. Kyushu University.

19. Fujishima, A., X. Zhang, and D.A. Tryk, *TiO2 photocatalysis and related surface phenomena.* Surface Science Reports, 2008. **63**(12): p. 515-582.

20. Fujishima, A., T.N. Rao, and D.A. Tryk, *Titanium dioxide photocatalysis.* Journal of Photochemistry and Photobiology C: Photochemistry Reviews, 2000. **1**(1): p. 1-21.

21. Fujishima, A., T.N. Rao, and D.A. Tryk, *TiO2 photocatalysts and diamond electrodes.* Electrochimica Acta, 2000. **45**(28): p. 4683-4690.

22. Hashimoto, K.I., H; Fujishima, A, *TiO2 photocataylsis: a historical overview and future prospects.* Japanese Journal of Applied Physics, 2005. **44**: p. 8269-8285.

23. Lee, S.-Y. and S.-J. Park, *TiO2 photocatalyst for water treatment applications.* Journal of Industrial and Engineering Chemistry, 2013. **19**(6): p. 1761-1769.

24. Matsunaga, T., et al., *Photoelectrochemical sterilization of microbial cells by semiconductor powders.* FEMS Microbiology Letters, 1985. **29**(1–2): p. 211-214.

25. Nakata, K. and A. Fujishima, *TiO2 photocatalysis: Design and applications.* Journal of Photochemistry and Photobiology C: Photochemistry Reviews, 2012. **13**(3): p. 169-189.

26. Herrmann, J.M., *Heterogeneous photocatalysis: state of the art and present applications In honor of Pr. R.L. Burwell Jr. (1912-2003), Former Head of Ipatieff Laboratories, Northwestern University, Evanston (Ill).* Topics in Catalysis, 2005. **34**(1-4): p. 49-65.

27. Zhang, W., L. Zou, and L. Wang, *Photocatalytic TiO2/adsorbent nanocomposites prepared via wet chemical impregnation for wastewater treatment: A review.* Applied Catalysis A: General, 2009. **371**(1–2): p. 1-9.

28. Alemany, L.J., et al., *Morphological and Structural Characterization of a Titanium Dioxide System.* Materials Characterization, 2000. **44**(3): p. 271-275.

29. Chen, X. and S.S. Mao, *Titanium Dioxide Nanomaterials: Synthesis, Properties, Modifications, and Applications.* Chemical Reviews, 2007. **107**(7): p. 2891-2959.

30. Pathakoti, K., et al., *Photoinactivation of Escherichia coli by Sulfur-Doped and Nitrogen-Fluorine-Codoped TiO2 Nanoparticles under Solar Simulated Light and Visible Light Irradiation.* Environ Sci Technol, 2013. **47**(17): p. 9988-96.

31. Hoffmann, M.M., Scot; Choi, Wonyong; Bahnemann, Detlef, *Environmental Applications of semiconductor Photocatalysis.* Chemistry, 1995. **95**: p. 69-96.

32. Berg, H., *Semiconductor Electrodes and Photoelectrochemistry: St. Licht (editor), Volume 6 of Encyclopedia of Electrochemistry, A. Bard, M. Stratmann (editors), Wiley-VCH, Weinheim, 2002, ISBN: 3-527-30398-7, X+597 pages, €349.00.* Bioelectrochemistry, 2003. **59**(1–2): p. 135.

33. Fujishima, A., X. Zhang, and D.A. Tryk, *Heterogeneous photocatalysis: From water photolysis to applications in environmental cleanup*. International Journal of Hydrogen Energy, 2007. **32**(14): p. 2664-2672.

34. Carvalho, J., *Caraterização e desenvolvimento de tintas para fotoinativação de microrganismos em meio aquoso*, in *Chemical Engineering*. 2013, Porto University. p. 76.

35. Magalhães, P., *Estudo e desenvolvimento de tintas para fotoinactivação de microrganismos para aplicações hospitalares*, in *Chemical Engineering*. 2011, Porto University. p. 51.

36. Chen, X., et al., *Doped semiconductor nanomaterials*. J Nanosci Nanotechnol, 2005. **5**(9): p. 1408-20.

37. Dworkin, M. and S. Falkow, *The Prokaryotes: Vol. 6: Proteobacteria: Gamma Subclass*. 2006: Springer.

38. Edberg, S.C., et al., *Escherichia coli: the best biological drinking water indicator for public health protection*. Symp Ser Soc Appl Microbiol, 2000(29): p. 106s-116s.

39. Castellani, A. and A.J. Chambers, *Manual of Tropical Medicine*. 1919: William Wood.

40. Blake, D.M., et al., *Application of the Photocatalytic Chemistry of Titanium Dioxide to Disinfection and the Killing of Cancer Cells*. Separation & Purification Reviews, 1999. **28**(1): p. 1-50.

41. Ireland, J.C., et al., *Inactivation of Escherichia coli by titanium dioxide photocatalytic oxidation*. Appl Environ Microbiol, 1993. **59**(5): p. 1668-70.

42. Kikuchi, Y., et al., *Photocatalytic bactericidal effect of TiO2 thin films: dynamic view of the active oxygen species responsible for the effect*. Journal of Photochemistry and Photobiology A: Chemistry, 1997. **106**(1–3): p. 51-56.

43. Maness, P.C., et al., *Bactericidal activity of photocatlytic TiO2 reaction: toward an understanding of its killing mechanism*. Applied and Environmental Microbiology, 1999. **65**: p. 4094-4098.

44. Sunada, K., T. Watanabe, and K. Hashimoto, *Studies on photokilling of bacteria on TiO2 thin film*. Journal of Photochemistry and Photobiology A: Chemistry, 2003. **156**(1–3): p. 227-233.

45. Willey, J.M., L.M. Sherwood, and C.J. Woolverton, *Prescott, Harley, and Klein's Microbiology*. 2008: McGraw-Hill Higher Education.

46. Buettner, G.R., B.A. Wagner, and C. Patrick Burns, *Free radical-mediated lipid peroxidation in cells: Oxidizability is a function of cell lipid vis-allylic hydrogen content*. Free Radical Biology and Medicine, 1993. **15**(5): p. 519.

47. Huang, Z., et al., *Bactericidal mode of titanium dioxide photocatalysis*. Journal of Photochemistry and Photobiology A: Chemistry, 2000. **130**(2–3): p. 163-170.

48. Lu, Z.-X., et al., *Cell Damage Induced by Photocatalysis of TiO2 Thin Films*. Langmuir, 2003. **19**(21): p. 8765-8768.

49. Matsunaga, T., et al., *Continuous-sterilization system that uses photosemiconductor powders*. Appl Environ Microbiol, 1988. **54**(6): p. 1330-3.

50. Águia, C., et al., *Influence of paint components on photoactivity of P25 titania toward NO abatement*. Polymer Degradation and Stability, 2011. **96**(5): p. 898-906.

51. Sousa, V.M., et al., *Photoinactivation of various antibiotic resistant strains of Escherichia coli using a paint coat*. Journal of Photochemistry and Photobiology A: Chemistry, 2013. **251**(0): p. 148-153.

52. Mills, A., C. Hill, and P.K.J. Robertson, *Overview of the current ISO tests for photocatalytic materials*. Journal of Photochemistry and Photobiology A: Chemistry, 2012. **237**(0): p. 7-23.

53. Gerhardt, P., *Methods for general and molecular bacteriology*. 1994, Washington, D.C.: American Society for Microbiology.

54. Dillert, R., U. Siemon, and D. Bahnemann, *Photocatalytic Disinfection of Municipal Wastewater*. Chemical Engineering & Technology, 1998. **21**(4): p. 356-358.

55. Ibáñez, J.A., M.I. Litter, and R.A. Pizarro, *Photocatalytic bactericidal effect of TiO2 on Enterobacter cloacae: Comparative study with other Gram (−) bacteria*. Journal of Photochemistry and Photobiology A: Chemistry, 2003. **157**(1): p. 81-85.

56. Tsai, T.-M., et al., *A comparative study of the bactericidal effect of photocatalytic oxidation by TiO2 on antibiotic-resistant and antibiotic-sensitive bacteria*. Journal of Chemical Technology & Biotechnology, 2010. **85**(12): p. 1642-1653.

57. Kozmin, S., et al., *UVA radiation is highly mutagenic in cells that are unable to repair 7,8-dihydro-8-oxoguanine in Saccharomyces cerevisiae*. Proceedings of the National Academy of Sciences of the United States of America, 2005. **102**(38): p. 13538-13543.

Appendix 1 – Design of feed system in solid works

Feed system solid works® design, create it in order to be manufacturate produced.

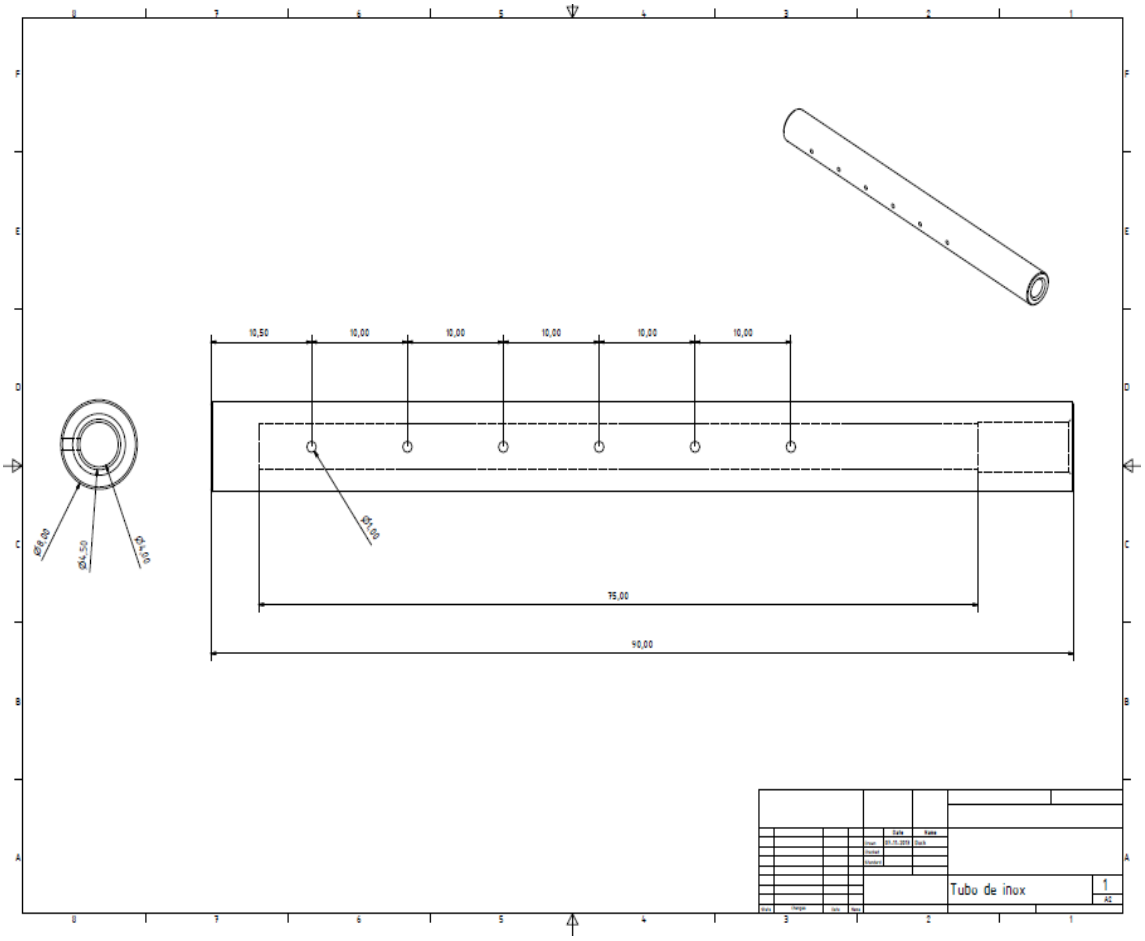

Figure 15. Design of feed system created in solid works®

Appendix 2 – Composition of PCA

The Plate Count Agar (PCA) was made by *Liofilchem*® in Italy, and its composition is shown:

Component	Quantity
Triptone	5,0 g/L
Glicose	1,0 g/L
Yeast extract	2,5 g/L
Agar	15,0 g/L
pH at 25°C	7,0 ± 0,2

Appendix 3 – Calculations to determined the quantity of TiO_2 contained in the coated mesh and the conversion to percentage weight/volume

Calculations to determine the real quantity of TiO_2 contained in the coated mesh, to carry out the maximum effiency photocatalytic system assay.

Table 3. Determining the weight of the mesh (2 x 2 mm^2) with and without photocatalytic paint.

Mesh with photocatalytic paint (g, ±0.001)	Mesh without photocatalytic paint (g, ±0.001)
1.030	0.900

The difference between the mesh painted and without paint coating gives the weight of the vinyl matt paint coating used.

1.030 – 0.900 = 0.130 g of paint coating

The TiO_2 contained in the formulation of vinyl matt was 9 wt.%. For instance, multiplying the weight of the paint coat obtained previously by 0.09 (representing the 9.0 % mentioned), its possible to obtained the quantity of TiO_2 immobilized.

0.130 * 0.09 = 0.012 g equivalent to 12 mg

In this matter, this quantity of TiO_2 was weight, then spreaded it in the most homogenized way along the surface area of the support mesh to be available to the ultraviolet lighting during the test and it was obtained 99.8 % of photoinactivation as it showed in the 4.2 photoinactivation procedure.

This photocatalys quantity expressed in percentage of weight/volume proceeds:

12 mg / 100 mL = 0.12 % w/v

Where 100 mL is the volume used for each photoinactivation assay.

Appendix 4 – Calculations to demonstrate the equivalence of the paint weight statistically

Validating two paint weight values statistically.

Table 4. Determining the weight of the mesh one (2 x 2 mm^2) with and without photocatalytic paint selected along the dissertation.

Mesh with photocatalytic paint (g, ±0.001)	Mesh without photocatalytic paint (g, ±0.001)	Photocatalytic paint (g, ±0.001)
10.719	11.084	0.365
10.719	11.083	0.364
10.720	11.082	0.362

Table 5. Determining the weight of the mesh two (2 x 2 mm^2) with and without photocatalytic paint selected along the dissertation.

Mesh with photocatalytic paint (g, ±0.001)	Mesh without photocatalytic paint (g, ±0.001)	Photocatalytic paint (g, ±0.001)
10.755	11.121	0.366
10.756	11.120	0.364
10.755	11.120	0.365

Resulst of t-test showed that the p value > α (level of significance), demonstrating that the weight values of the two random mesh selected are not statistically different.

Appendix 5 - Calculations to determine the quantity of cycles of the water using different flow rates, 1, 2 and 4 $mL \cdot s^{-1}$.

Cycle equation:

$$cycle = \frac{Q}{V} * t$$

Where Q is the flow rate ($mL \cdot s^{-1}$), V is the volume (mL), t is the irradiation time (min).

Calculations to determine the quantity of cycles of the liquid on the close and recirculated photocatalytic system when a photoinactivation assay is carry out using a flow rate of 2 $mL \cdot s^{-1}$, 100 mL of cell suspension for 40 min.

$$40\ \text{min}\ x\ \frac{60s}{1\ min}\ x\ \frac{2mL}{1s}\ x\ \frac{1}{100mL} = 48\ turns$$

For the case where the flow rate is double inferior, the quantity of turns is double inferior as well, as shown in next:

$$40\ \text{min}\ x\ \frac{60s}{1\ min}\ x\ \frac{1mL}{1s}\ x\ \frac{1}{100mL} = 24\ turns$$

For the case where the flow rate is double higher, the quantity of turns is double higher as well, as shown in next:

$$40\ \text{min}\ x\ \frac{60s}{1\ min}\ x\ \frac{4mL}{1s}\ x\ \frac{1}{100mL} = 96\ turns$$

For the case where the assay time is double, the quantity of turns is double higher as well, as shown in next:

$$80\ \text{min}\ x\ \frac{60s}{1\ min}\ x\ \frac{2mL}{1s}\ x\ \frac{1}{100mL} = 96\ turns$$

Appendix 6 - Calculations to determine the residence time of the contaminated water using 1 mL·s-1, 2 mL·s-1 and 4 mL·s-1 of flow rate.

Residence time equation:

$$\tau = \frac{Q}{V}$$

Tau (τ) is the residence time (s^{-1}), Q is the flow rate ($mL \cdot s^{-1}$), V is the volume (mL).

Applying the equation of residence time to the configuration of 1 $mL \cdot s^{-1}$ flow rate, as shown in:

$$\tau = \frac{1\ \mathrm{mL \cdot s^{-1}}}{100mL} = 0.01\ \mathrm{s^{-1}}$$

Applying the equation residence of time to the configuration of 2 $mL \cdot s^{-1}$ flow rate, as shown in:

$$\tau = \frac{2\ \mathrm{mL \cdot s^{-1}}}{100mL} = 0.02\ \mathrm{s^{-1}}$$

Applying the equation residence of time to the configuration of 4 $mL \cdot s^{-1}$ flow rate, as shown in:

$$\tau = \frac{4\ \mathrm{mL \cdot s^{-1}}}{100\ mL} = 0.04\ \mathrm{s^{-1}}$$

Appendix 7 - Calculations to estimate the effective area of the stainless steel mesh of 2 x 2 mm^2 and 3 x 3 mm^2

A estimative mathematical method to obtained the effective area of the mesh is proposed by the author of this thesis.

Defining 4 types of areas: total (A_T), effective (A_{ef}), empty (A_e) and hole (A_h).

The total area reach the complete area taking the mesh dimensions (6 cm width x 16 cm length), applying for both cases.

The total area is calculated as shown in equation:

$$A_T = w * l$$

Where w is width and l is length

$$A_T = 16 * 6 \text{ cm} = 96 \text{ cm}^2$$

For the 2 x 2 mm^2 and 3 x 3 mm^2 stainless steel meshes the definition for A_{ef}, A_e and A_h are different.

Firstly, calculate the hole area, as shown in equation:

$$A_h = s * s$$

Where s is the side

$$A_h = 0.2 * 0.2 = 0.04 \text{ cm}^2$$

Secondly, calculate the number of holes existing in the 2 x 2 mm^2 approximately 1364.

Thirdly, calculate the empty area, as shown in equation:

$$A_e = \text{holes number} * A_h$$

$$A_e = 1364 * 0.04 \text{ cm}^2 = 54.56 \text{ cm}^2$$

Finally, calculate the effective-available area of the mesh, as shown in equation:

$$A_{ef} = A_T - A_e$$

$$A_{ef} = (96 - 54.56) \text{ cm}^2 = 41.44 \text{ cm}^2$$

For the 3 x 3 mm^2 mesh had followed the same equation presented above. With the exception of some values are different. The number of holes were approximately 864. For instance, calculating the hole area, empty area and effective-available area of the mesh as shown in next equations:

$$A_h = 0.3 * 0.3 = 0.09\ cm^2$$

$$A_e = 864 * 0.09 = 77.76\ cm^2$$

$$A_{ef} = (96.00 - 77.76)\ cm^2 = 18.24\ cm^2$$

Appendix 8 – Statistical analysis

a) Statistical analysis for different materials applying the One-way ANOVA by the Tukey at $p < 0.05$, using the R™ statistical computing and graphics software develope by Bell Laboratories.

Material	% Viability loss	
Plastic (2x2 mm^2)	38.16568047	a
Plastic (2x2 mm^2)	38.73015873	a
Plastic (2x2 mm^2)	38.41059603	a
Stainless steel (2x2 mm^2)	51.31578947	b
Stainless steel (2x2 mm^2)	58.808933	b
Stainless steel (2x2 mm^2)	52.30263158	b
Stainless steel (3x3 mm^2)	41.6988417	a
Stainless steel (3x3 mm^2)	32.25806452	a
Stainless steel (3x3 mm^2)	37.09677419	a
Pure TiO_2	99.84100418	c
Pure TiO_2	99.83448276	c
Pure TiO_2	99.73863636	c

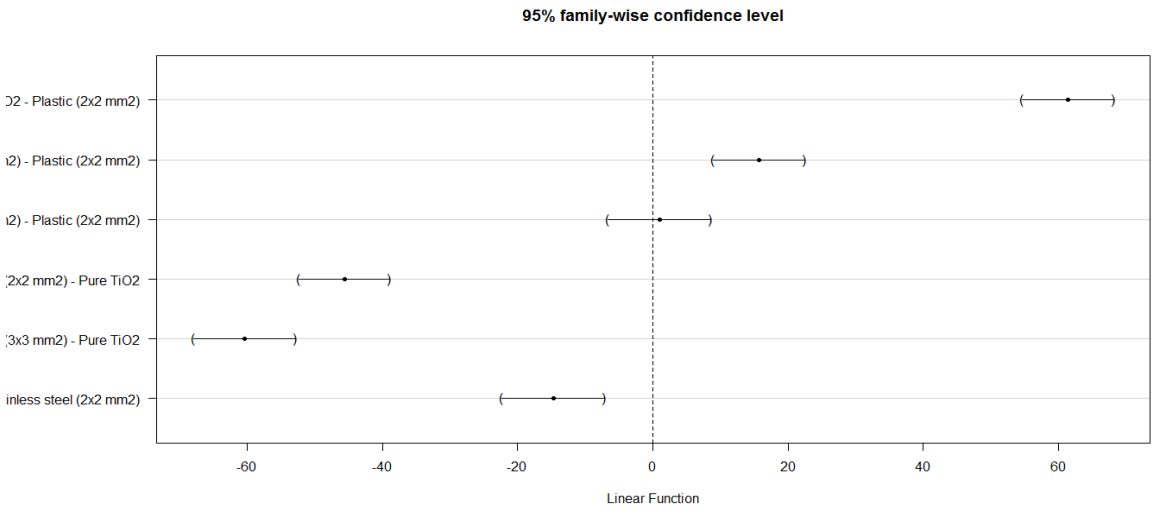

b) Statistical analysis for two changeable flow rates applying the One-way ANOVA by the Tukey at $p < 0.05$, using the R™ statistical computing and graphics software develope by Bell Laboratories.

Flow rate	Means	
40 min, 4 $mL \cdot s^{-1}$	43.4131737	b
40 min, 4mL/s	40.7692308	b
40 min, 4mL/s	38.5665529	b
40 min, 2mL/s	51.3157895	c
40 min, 2mL/s	58.808933	c
40 min, 2mL/s	52.3026316	c
40 min, 1mL/s	19.7969543	a
40 min, 1mL/s	10.7954545	a
40 min, 1mL/s	11.1111111	a

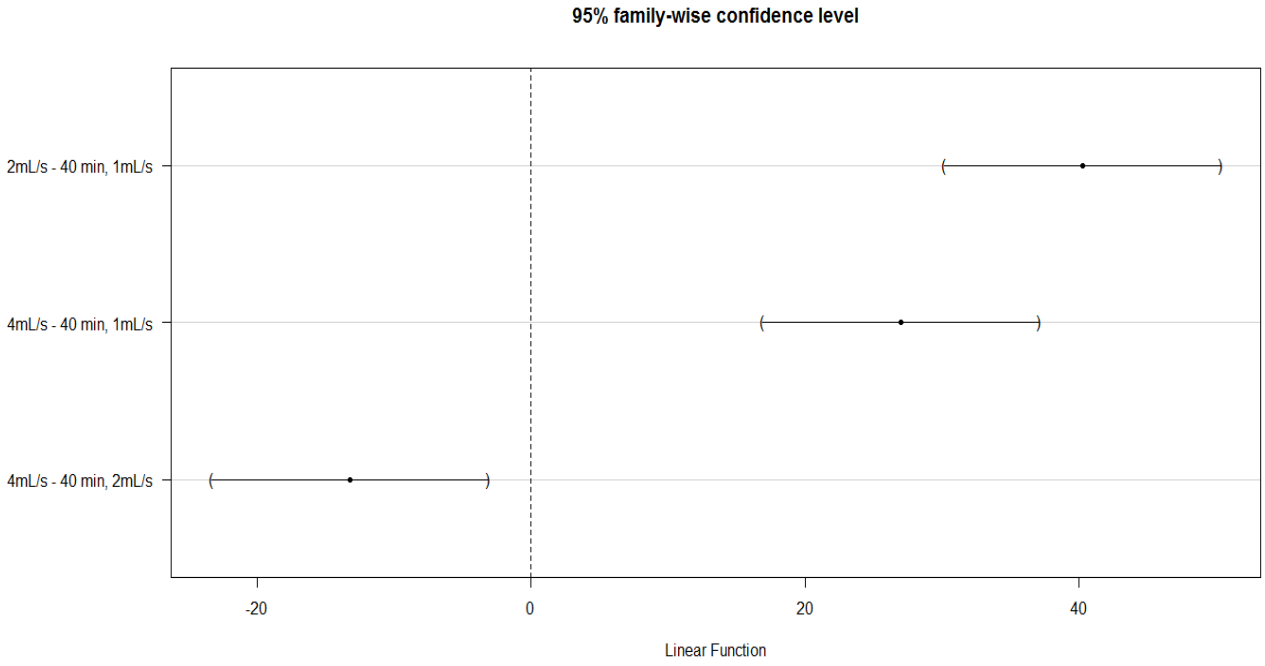

c) Statistical analysis for the variables: materials, flow rate, irradiation time and reproducibility, presented in the $\log_{10}$ CFU mL^{-1} graphic. Applying the One-way ANOVA by the Tukey at $p < 0.05$, using the R™ statistical computing and graphics software develope by Bell Laboratories.

Variable	Mean Log UFC/ml	
Pure TiO_2 - i	6.07736791	fg
Pure TiO_2 - i	6.161368	fg
Pure TiO_2 - i	6.12057393	fg
Pure TiO_2 - f	3.2787536	a
Pure TiO_2 - f	3.38021124	a
Pure TiO_2 - f	3.5378191	a
1.Stainless steel (2x2 mm^2) -i	6.18184359	g
1.Stainless steel (2x2 mm^2) -i	6.30427505	g
1.Stainless steel (2x2 mm^2) -i	6.18184359	g
1.Stainless steel (2x2 mm^2) -f	5.86923172	d
1.Stainless steel (2x2 mm^2) -f	5.91907809	d
1.Stainless steel (2x2 mm^2) -f	5.86033801	d
2.Stainless steel (2x2 mm^2) -i	6.07918125	def
2.Stainless steel (2x2 mm^2) -i	5.8893017	def
2.Stainless steel (2x2 mm^2) -i	5.96614173	def
2.Stainless steel (2x2 mm^2) -f	5.70757018	c
2.Stainless steel (2x2 mm^2) -f	5.59106461	c
2.Stainless steel (2x2 mm^2) -f	5.64345268	c
Stainless steel (3x3 mm^2) -i	6.11226977	eg
Stainless steel (3x3 mm^2) -i	6.09342169	eg
Stainless steel (3x3 mm^2) -i	6.09342169	eg
Stainless steel (3x3 mm^2) -f	5.87794695	d
Stainless steel (3x3 mm^2) -f	5.92427929	d
Stainless steel (3x3 mm^2) -f	5.8920946	d
Plastic (2x2 mm^2) -i	6.2278867	g
Plastic (2x2 mm^2) -i	6.19728056	g
Plastic (2x2 mm^2) -i	6.17897695	g
Plastic (2x2 mm^2) -f	6.01911629	def
Plastic (2x2 mm^2) -f	5.98452731	def
Plastic (2x2 mm^2) -f	5.96848295	def
40 min, 4 $mL \cdot s^{-1}$-i	6.22271647	g
40 min, 4 $mL \cdot s^{-1}$ -i	6.11394335	g
40 min, 4 $mL \cdot s^{-1}$ -i	6.16583762	g
40 min, 4 $mL \cdot s^{-1}$ -f	5.97543181	de
40 min, 4 $mL \cdot s^{-1}$ -f	5.88649073	de

40 min, 4 mL·s^{-1} -f	5.95424251	de
40 min, 1 mL·s^{-1} -i	5.99343623	de
40 min, 1 mL·s^{-1} -i	5.94448267	de
40 min, 1 mL·s^{-1} -i	5.90848502	de
40 min, 1 mL·s^{-1} -f	5.89762709	d
40 min, 1 mL·s^{-1} -f	5.89486966	d
40 min, 1 mL·s^{-1} -f	5.8573325	d
80 min, 2 mL·s^{-1} -i	5.88081359	de
80 min, 2 mL·s^{-1} -i	5.99343623	de
80 min, 2 mL·s^{-1} -i	5.95424251	de
80 min, 2 mL·s^{-1} -f	4.95182304	b
80 min, 2 mL·s^{-1} -f	4.96614173	b
80 min, 2 mL·s^{-1} -f	4.98227123	b

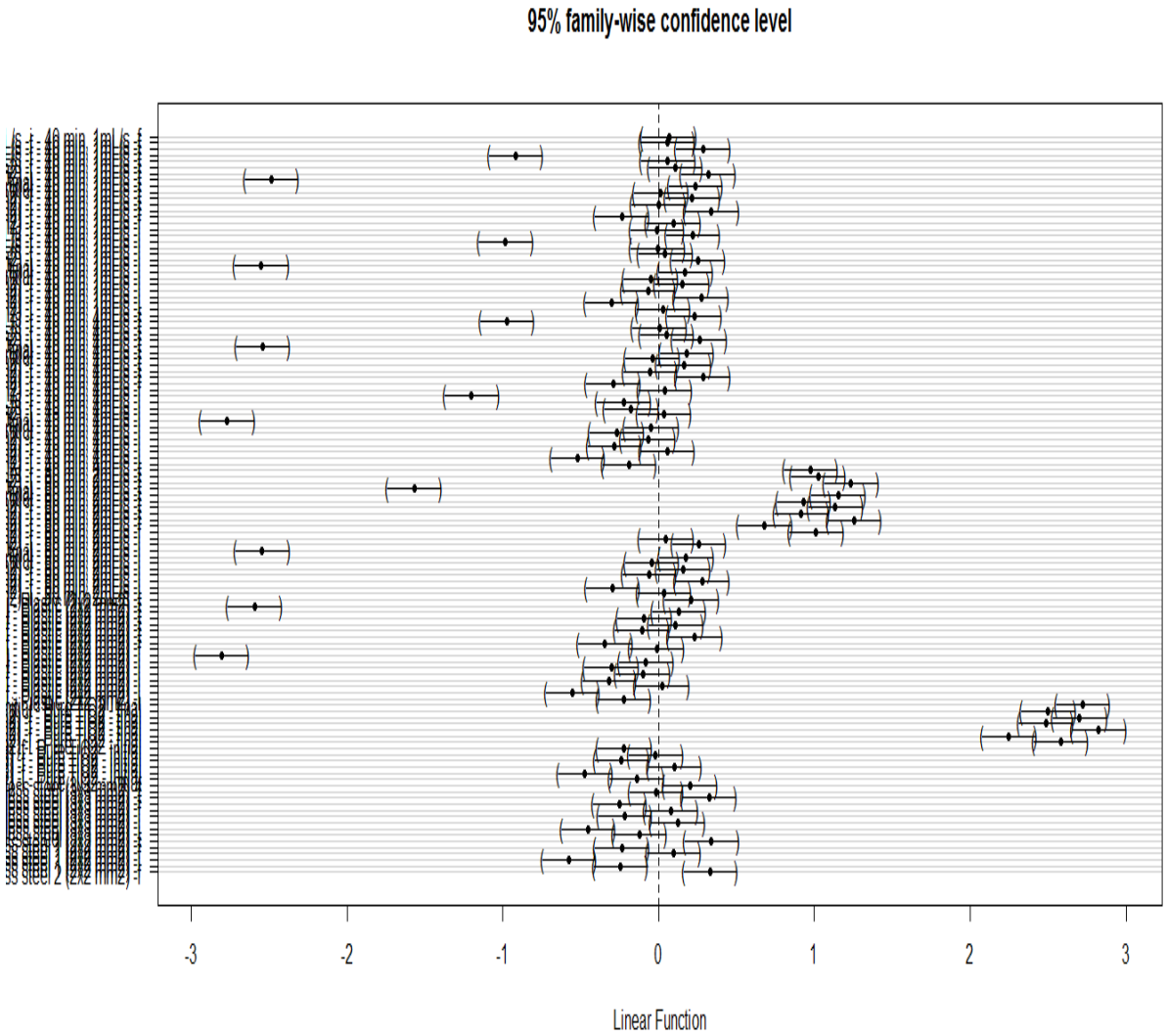

d) Statistical analysis for pure TiO_2 photocatalysis, UV-A and dark control applying the One-way ANOVA by the Tukey at $p < 0.05$, using the R™ statistical computing and graphics software develope by Bell Laboratories.

	% Viability loss	
Pure TiO_2	99.738636	C
Pure TiO_2	99.834483	C
Pure TiO_2	99.841004	C
UV light only % viability loss	30.718954	B
UV light only % viability loss	26.804124	B
UV light only % viability loss	29.714286	B
TiO_2 (P25) in dark conditions	5.3278689	A
TiO_2 (P25) in dark conditions	7.860262	A
TiO_2 (P25) in dark conditions	-1.515152	A

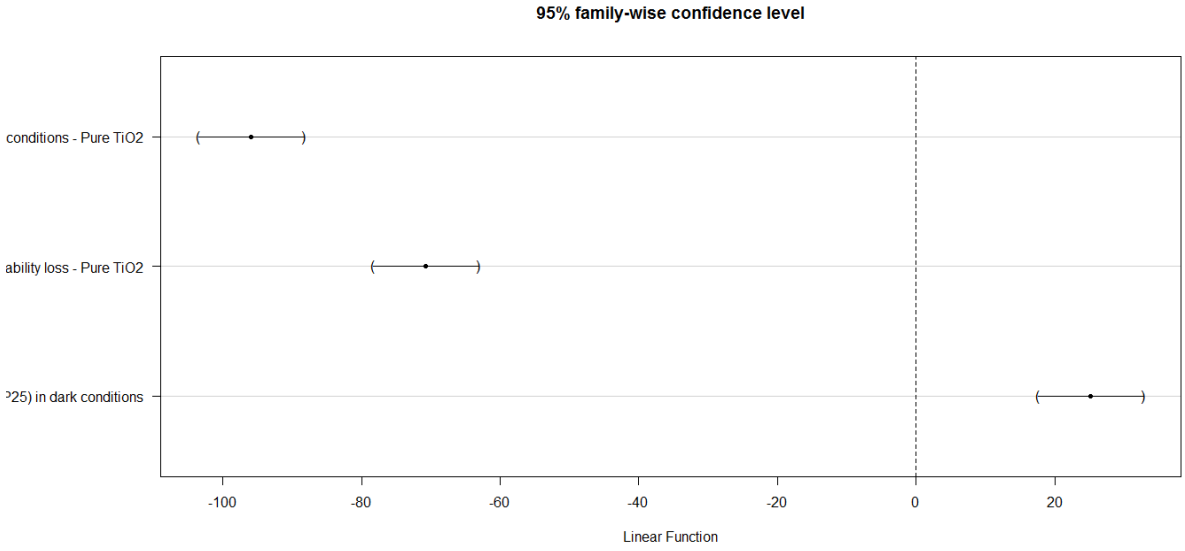

e) Statistical analysis for first Stainless steel (2 x 2 mm^2) photocatalysis, UV-A and dark controls applying the One-way ANOVA by the Tukey at $p < 0.05$, using the R™ statistical computing and graphics software develope by Bell Laboratories.

	% Viability loss	
Stainless steel (2x2 mm^2)	51.31578947	B
Stainless steel (2x2 mm^2)	58.808933	B
Stainless steel (2x2 mm^2)	52.30263158	B
UV light only % viability loss	7.142857143	A
UV light only % viability loss	4.736842105	A
UV light only % viability loss	12.54752852	A
TiO_2 (P25) in dark conditions	0	A
TiO_2 (P25) in dark conditions	0	A
TiO_2 (P25) in dark conditions	0	A

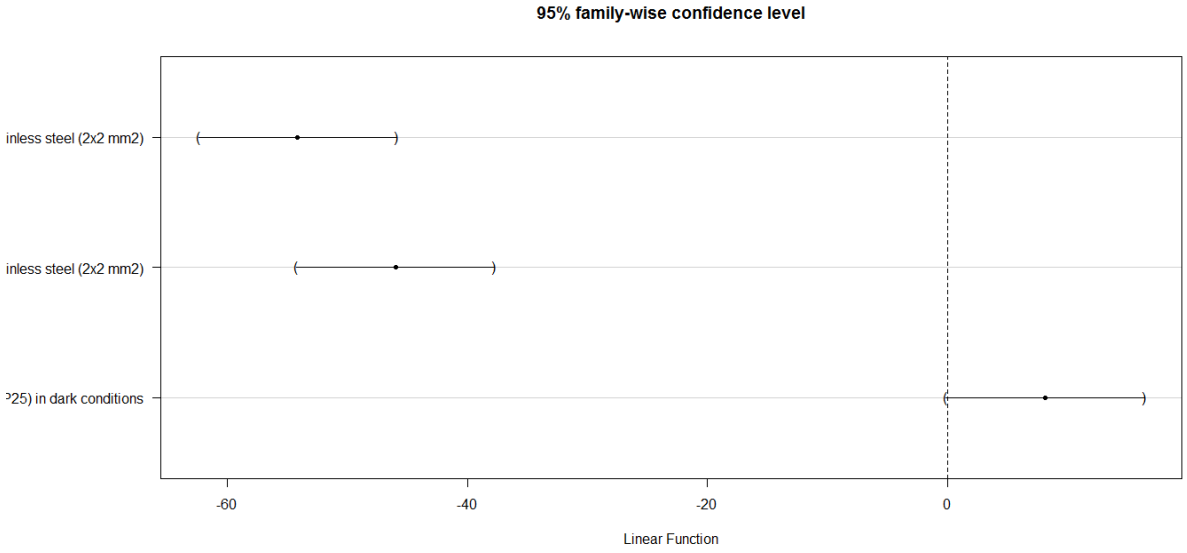

f) Statistical analysis for second Stainless steel (2 x 2 mm2) photocatalysis, UV-A and dark controls applying the One-way ANOVA by the Tukey at $p < 0.05$, using the R™ statistical computing and graphics software develope by Bell Laboratories.

Material	% Viability loss	
1.Stainless steel (2x2 mm^2)	51.31578947	B
1.Stainless steel (2x2 mm^2)	58.808933	B
1.Stainless steel (2x2 mm^2)	52.30263158	B
UV light only % viability loss	7.142857143	A
UV light only % viability loss	4.736842105	A
UV light only % viability loss	12.54752852	A
TiO_2 (P25) in dark conditions	0	A
TiO_2 (P25) in dark conditions	0	A
TiO_2 (P25) in dark conditions	0	A

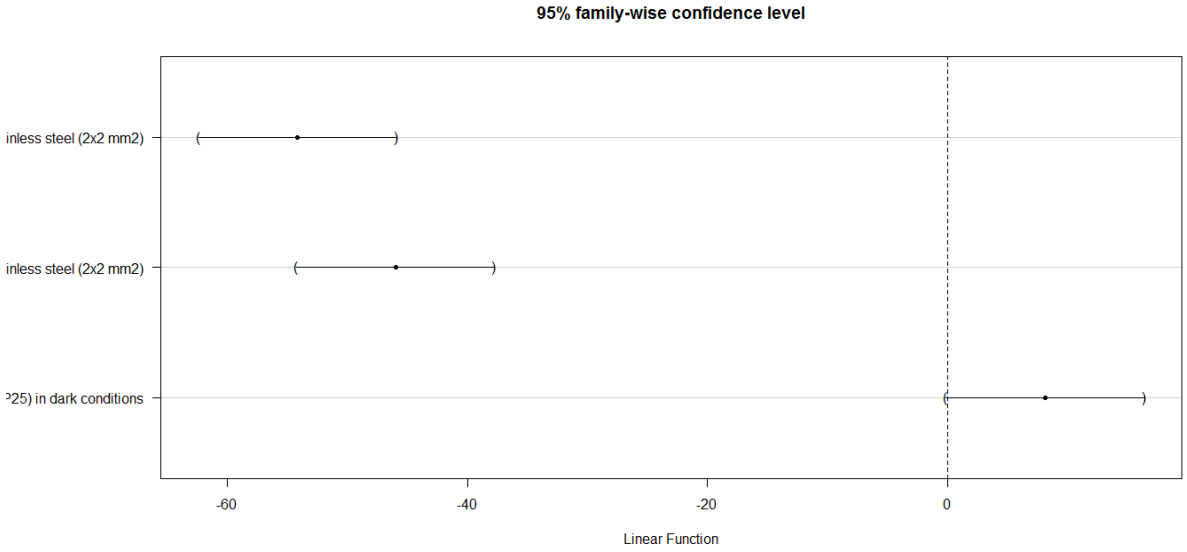

g) Statistical analysis for Stainless steel (3 x 3 mm^2) photocatalysis, UV-A and dark controls applying the One-way ANOVA by the Tukey at $p < 0.05$, using the R™ statistical computing and graphics software develope by Bell Laboratories.

	% Viability loss	
Stainless steel (3x3 mm^2)	41.698842	A
Stainless steel (3x3 mm^2)	32.258065	A
Stainless steel (3x3 mm^2)	37.096774	A
UV light only % viability loss	30.19943	B
UV light only % viability loss	13.253012	B
UV light only % viability loss	10.738255	B
TiO_2 (P25) in dark conditions	0	C
TiO_2 (P25) in dark conditions	0	C
TiO_2 (P25) in dark conditions	0	C

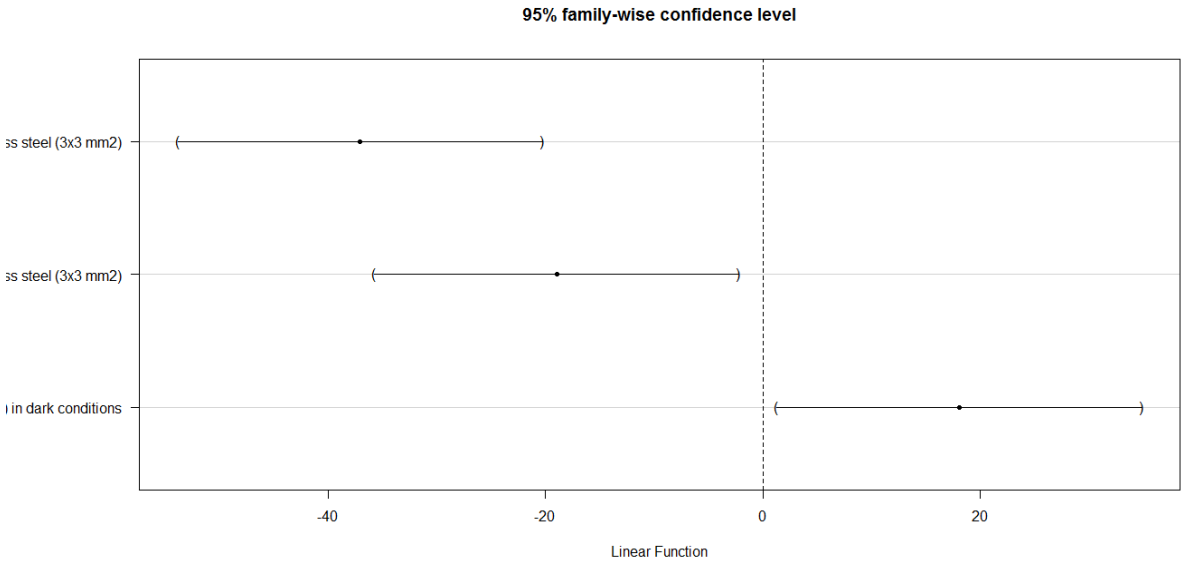

h) Statistical analysis for flow rate of 4 $mL \bullet s^{-1}$ photocatalysis, UV-A and dark controls applying the One-way ANOVA by the Tukey at $p < 0.05$, using the R™ statistical computing and graphics software develope by Bell Laboratories.

Flow rate	% Viability loss	
40 min, 4 $mL \bullet s^{-1}$	43.41317365	A
40 min, 4 $mL \bullet s^{-1}$	40.76923077	A
40 min, 4 $mL \bullet s^{-1}$	38.5665529	A
UV light only % viability loss	30.1994302	B
UV light only % viability loss	13.25301205	B
UV light only % viability loss	10.73825503	B
TiO_2 (P25) in dark conditions	0	C
TiO_2 (P25) in dark conditions	0	C
TiO_2 (P25) in dark conditions	0	C

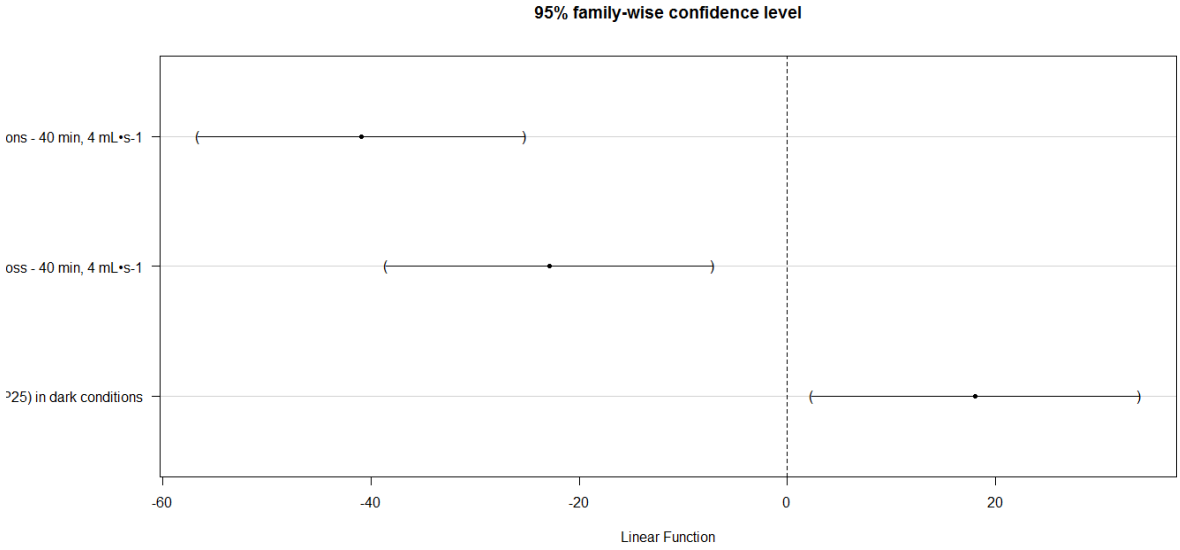

i) Statistical analysis for irradiation time of 80 min photocatalysis, UV-A and dark controls applying the One-way ANOVA by the Tukey at $p < 0.05$, using the R™ statistical computing and graphics software develope by Bell Laboratories.

Flow rate	% Viability loss	C
80 min, 2 mL•s^{-1}	88.22368421	C
80 min, 2 mL•s^{-1}	90.60913706	C
80 min, 2 mL•s^{-1}	89.33333333	B
UV light only % viability loss	33.17307692	B
UV light only % viability loss	36.31578947	B
TiO_2 (P25) in dark conditions	0	A
TiO_2 (P25) in dark conditions	0	A
TiO_2 (P25) in dark conditions	0	A

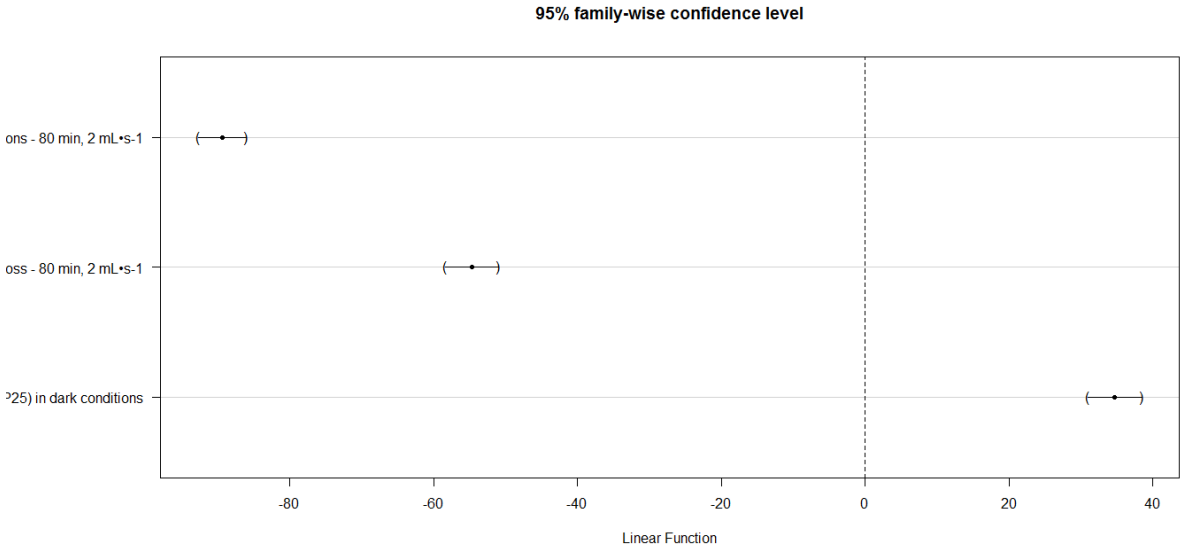

j) Statistical analysis for different flow rates applying the two sample t-test at $p < 0.05$ using the Excel™ data statistical analysis.

Assay time	% Viability loss	
40 min, 2 $mL \bullet s^{-1}$	51.31578947	A
40 min, 2 $mL \bullet s^{-1}$	58.808933	A
40 min, 2 $mL \bullet s^{-1}$	52.30263158	A
80 min, 2 $mL \bullet s^{-1}$	88.22368421	B
80 min, 2 $mL \bullet s^{-1}$	90.60913706	B
80 min, 2 $mL \bullet s^{-1}$	89.33333333	B

t-Test: Two-Sample Assuming Equal Variances		
	Variable 1	Variable 2
Mean	54.142451	89.388718
Variance	16.575503	1.4248969
Observations	3	3
Pooled Variance	9.0001998	
Hypothesized Mean Difference	0	
Df	4	
t Stat	-14.38907	
P(T<=t) one-tail	6.779E-05	
t Critical one-tail	2.1318468	
P(T<=t) two-tail	0.0001356	
t Critical two-tail	2.7764451	

The values are significantly different

k) Statistical analysis for different flow rates applying the two sample t-test at $p < 0.05$ using the Excel™ data statistical analysis.

Flow rate	% Viability loss	
40 min, 4 mL•s-1	43.41317365	b
40 min, 4 mL•s-1	40.76923077	b
40 min, 4 mL•s-1	38.5665529	b
40 min, 2 mL•s-1	51.31578947	c
40 min, 2 mL•s-1	58.808933	c
40 min, 2 mL•s-1	52.30263158	c
40 min, 1 mL•s-1	19.79695431	a
40 min, 1 mL•s-1	10.79545455	a
40 min, 1 mL•s-1	11.11111111	a

t-Test: Two-Sample Assuming Equal Variances

	Variable 1	*Variable 2*
Mean	54.1424514	89.3887182
Variance	16.5755026	1.42489693
Observations	3	3
Pooled Variance	9.00019976	
Hypothesized Mean Difference	0	
Df	4	
t Stat	-14.3890685	
P(T<=t) one-tail	6.7785E-05	
t Critical one-tail	2.13184679	
P(T<=t) two-tail	0.00013557	
t Critical two-tail	2.77644511	

The values are significantly different

l) Statistical analysis for evaluate the reproducibility of two repeat assays applying the two sample t-test at $p < 0.05$ using the Excel™ data statistical analysis.

Reproducibility	% Viability loss	
40 min, 2 mL•s-1	51.315789	A
40 min, 2 mL•s-1	58.808933	A
40 min, 2 mL•s-1	52.302632	A
40 min, 2 mL•s-1	57.5	A
40 min, 2 mL•s-1	49.677419	A
40 min, 2 mL•s-1	52.432432	A

t-Test: Two-Sample Assuming Equal Variances

	Variable 1	*Variable 2*
Mean	54.1424514	53.2032839
Variance	16.5755026	15.743851
Observations	3	3
Pooled Variance	16.1596768	
Hypothesized Mean Difference	0	
df	4	
t Stat	0.28613588	
P(T<=t) one-tail	0.39449079	
t Critical one-tail	2.13184679	
P(T<=t) two-tail	0.78898158	
t Critical two-tail	2.77644511	

The values are not significantly different